

1 **Short title:** *NbMORF8* negatively regulates plant immunity

2 **Corresponding author:** Weixing Shan, wxshan@nwafu.edu.cn

3

4 **Cytidine-to-Uridine RNA editing factor NbMORF8 negatively regulates plant immunity to**
5 ***Phytophthora* pathogens**

6

7 Yang Yang¹, Guangjin Fan^{2,3}, Yan Zhao¹, Qujiang Wen², Peng Wu², Yuling Meng¹, Weixing
8 Shan^{1*}

9 ¹State Key Laboratory of Crop Stress Biology for Arid Areas and College of Agronomy,
10 Northwest A&F University, Yangling, Shaanxi 712100, China;

11 ²State Key Laboratory of Crop Stress Biology for Arid Areas and College of Plant Protection,
12 Northwest A&F University, Yangling, Shaanxi 712100, China;

13 ³Present address: College of Plant Protection, Southwest University

14

15 ***Correspondence:** wxshan@nwafu.edu.cn

16

17 **One-sentence summary:** A mitochondrion- and chloroplast-targeted RNA editing factor
18 negatively regulates plant immunity to *Phytophthora* pathogens by suppressing effector
19 accumulation, ROS burst, and SA signaling.

20

21 **Author contributions:** W.S., Y.Y., and Y.M. conceived and designed the experiments. Y.Y.,
22 G.F., Y.Z., Q.W., and P.W. performed the experiments. Y.Y. and W.S. analyzed the data. Y.Y.,
23 Y.M., and W.S. wrote the manuscript. All authors reviewed the manuscript. W.S. agrees to serve
24 as the author responsible for contact and ensures communication.

25

26 **Funding information:** This work was supported by China Agriculture Research System
27 (CARS-09), National Natural Science Foundation of China (31125022 and 31930094), and the
28 Program of Introducing Talents of Innovative Discipline to Universities (project 111) from the
29 State of Administration for Foreign Experts Affairs, P. R. China (B18042).

30

31 **Abstract**

32 Mitochondria and chloroplasts play key roles in plant-pathogen interactions. Cytidine-to-uridine
33 (C-to-U) RNA editing is a critical post-transcriptional modification in mitochondria and
34 chloroplasts that is specific to flowering plants. Multiple organellar RNA editing factors
35 (MORFs) form a protein family that participates in C-to-U RNA editing, but little is known
36 regarding their immune functions. Here, we report the identification of *NbMORF8*, a negative
37 regulator of plant immunity to *Phytophthora* pathogens. Using virus-induced gene silencing
38 (VIGS) and transient expression in *Nicotiana benthamiana*, we show that *NbMORF8* functions
39 through regulation of ROS production, SA signaling, and accumulation of multiple RXLR
40 effectors of *Phytophthora* pathogens. NbMORF8 is localized to mitochondria and chloroplasts,
41 and its immune function requires mitochondrial targeting. The conserved MORF box domain is
42 not required for its immune function. Furthermore, we show that the preferentially mitochondrial
43 localized NbMORF proteins negatively regulate plant resistance against *Phytophthora*, whereas
44 the preferentially chloroplast localized ones are positive immune regulators. Our study reveals
45 that the C-to-U RNA editing factor *NbMORF8* negatively regulates plant immunity to the
46 oomycete pathogen *Phytophthora*, and that mitochondrial and chloroplast localized NbMORF
47 family members exert opposing effects on immune regulation.

48

49 **Keywords**

50 MORF proteins, plant immunity, RNA editing, oomycete, *Phytophthora*, plant susceptibility,
51 RXLR effectors

52

53 **Introduction**

54 Mitochondria and chloroplasts, which serve as energy conversion sites within cells, play
55 key roles in plant-pathogen interactions. Mitochondria and chloroplasts are important sources of
56 reactive oxygen species (ROS), which may act as key defense molecules in plant immune
57 responses and as signaling molecules during the spread of the hypersensitive response
58 (Amirsadeghi et al., 2007; Colombatti et al., 2014). Production of several plant hormones
59 involved in immunity, e.g. jasmonic acid (JA), salicylic acid (SA), and abscisic acid, depends on
60 chloroplast metabolism (Apel and Hirt, 2004; Mittler et al., 2004; Nomura et al., 2012; Serrano
61 et al., 2016). Due to the significant role played by mitochondria and chloroplasts in plant

62 immunity, plant pathogens secrete many virulence effectors that are targeted to chloroplasts and
63 mitochondria to modulate their effect on host immunity (Block et al., 2010; Rodriguez-Herva et
64 al., 2012; de Torres Zabala et al., 2015). However, it remains largely unclear how mitochondrial
65 and chloroplast proteins achieve modulation of the plant immune system.

66 Cytidine-to-uridine (C-to-U) RNA editing in mitochondria and chloroplasts, which is
67 mainly regulated by nuclear-encoded RNA editing factors, is a critical post-transcriptional
68 modification specific to flowering plants (Gray and Covello, 1993; Takenaka et al., 2013; Barkan
69 and Small, 2014; Shikanai, 2015; Yan et al., 2017). C-to-U RNA editing usually changes the first
70 or second positions of nucleic acid triplet codons leading to altered protein sequences. Five
71 groups of proteins participating in C-to-U RNA editing have been identified: pentatricopeptide
72 repeat (PPR) proteins, multiple organelle RNA editing factors (MORFs, also known as
73 RNA-editing factor interacting proteins (RIPs)), organelle RNA recognition motif-containing
74 (ORRM) proteins, protoporphyrinogen IX oxidase 1 (PPO1), and organelle zinc finger 1 (OZ1)
75 (Zhang et al., 2014; Sun et al., 2015; Sun et al., 2016; Yan et al., 2017). Increasing evidence
76 supports the conclusion that this type of post-transcriptional modification plays important roles
77 in plant metabolism, adaptations to the environment, and signal transduction (Zsigmond et al.,
78 2008; Yan et al., 2017; Yang et al., 2017; He et al., 2018).

79 PPR proteins directly interact with mRNA to determine the specificity of RNA editing and a
80 PPR protein specifically recognizes one or several editing sites (Barkan and Small, 2014). In
81 land plants, the PPR family is greatly expanded, e.g. *Arabidopsis* (*Arabidopsis thaliana*) contains
82 more than 400 PPR proteins, whereas there are much few PPR proteins in fungi, protists, and
83 animals (Barkan and Small, 2014). In contrast, the MORF family only has nine members in
84 *Arabidopsis*: two MORFs are targeted to plastids (AtMORF2 and AtMORF9), six are targeted to
85 mitochondria (AtMORF1, AtMORF3, AtMORF4, AtMORF5, AtMORF6, and AtMORF7), and
86 one (AtMORF8) localizes to both organelles (Bentolila et al., 2012; Takenaka et al., 2012). The
87 role of MORFs is to interact with other RNA editing factors to form an RNA editosome
88 (Bentolila et al., 2012; Hartel et al., 2013; Takenaka et al., 2013; Brehme et al., 2015; Glass et
89 al., 2015; Hackett et al., 2017; Ma et al., 2017). For example, MORF8 has been shown to be a
90 component in multiple editing complexes. Unlike the PPR proteins, each MORF protein
91 participates in multiple RNA editing sites. In addition, MORFs usually form homomers or
92 heteromers to aid in editosome formation (Zehrmann et al., 2015). Sequence alignment of all

93 nine known MORF family proteins in Arabidopsis showed that they share a conserved motif, the
94 so-called MORF box, which is approximately 100 amino acid residues from the N-terminus of
95 the protein (Takenaka et al., 2012). Given the large number of RNA editing factors (~400 PPR
96 proteins, 9 MORFs, and 6 ORRMs in Arabidopsis (Yan et al., 2017)), our understanding of their
97 roles in regulating plant immunity is limited. To date, there has only been one report on the role
98 of RNA editing related factors in plant immunity, that being for the Arabidopsis
99 chloroplast-located protein OCP3, which regulates resistance to the necrotrophic pathogen
100 *Plectosphaerella cucumerina* by regulating the RNA editing of the chloroplast gene *ndhB*
101 (Garcia-Andrade et al., 2013).

102 To detect and respond to invading pathogens, plants have evolved pattern recognition
103 receptors (PRRs) to recognize conserved pathogen- or microbe-associated molecular patterns
104 (PAMPs or MAMPs) (Jones and Dangl, 2006). PAMP-triggered immunity (PTI) is the basal
105 immune response to broad-spectrum pathogens. To overcome this basal immune system,
106 pathogens have developed a variety of effectors. In turn, plants have developed a second group
107 of receptors, nucleotide binding-leucine rich repeat receptors (NLR), to detect the presence of
108 effectors, resulting in effector-triggered immunity (ETI) (Jones and Dangl, 2006). Effectors can
109 be directly or indirectly recognized by corresponding NLR proteins leading to strong and fast
110 cell death, called the hypersensitive response (HR), hence restricting pathogen growth (Jones and
111 Dangl, 2006; Schwessinger and Ronald, 2012). The effectors that are recognized by the NLR
112 proteins are called avirulence (AVR) proteins. Many *Avr* and *R* gene pairs have been cloned
113 from *Phytophthora* pathogens and their hosts, e.g. *P. infestans* *Avr* genes *PiAvr3a* (Armstrong et
114 al., 2005), *PiAvrblb1* (Vleeshouwers et al., 2008), and *PiAvrVnt1* (Pel et al., 2009), and
115 corresponding potato *R* genes *R3a* (Huang et al., 2005), *RB* (Song et al., 2003), and *RpiVnt1*
116 (Foster et al., 2009).

117 *Phytophthora* represent a unique group of plant pathogens called oomycetes that are
118 phylogenetically distant from true fungi. Nearly all 120 *Phytophthora* species identified in the
119 genus are plant pathogens, capable of infecting hundreds of plant species including many
120 important crops and causing devastating diseases leading to huge economic losses every year
121 (Kamoun et al., 2015). The most well-known is *P. infestans*, the causal agent of potato late blight
122 and the Great Irish Famine in the 19th century. While recognition of pathogen effectors is
123 genetically well known and molecularly well characterized, and widely used for development of

124 genotype-specific disease resistance, little is known about the genetic basis of plant susceptibility
125 to *Phytophthora* pathogens.

126 Analysis of the roles of *MORF* genes, beyond their RNA editing function, has been
127 hampered by lethal or growth retardation consequences resulting from their *in planta* expression
128 suppression. In this study, we employ virus-induced gene silencing (VIGS) and *Agrobacterium*
129 *tumefaciens*-mediated transient expression in *Nicotiana benthamiana* to investigate the immune
130 function of *NbMORF* genes that were responsive to infection by *P. parasitica*. We show that
131 NbMORF8 was localized in chloroplasts and mitochondria and played a substantial role in
132 immunity by negatively regulating plant resistance against *Phytophthora* pathogens. Its immune
133 function involves regulation of ROS burst and the SA signaling pathway, and accumulation of
134 multiple RXLR (Arg-X-Leu-Arg) effectors of *Phytophthora* pathogens. Furthermore, we found
135 that the immune function of *NbMORF8* is independent of its conserved MORF box domain. We
136 also found that mitochondrion-preferred NbMORF proteins (NbMORF1a and NbMORF1b)
137 negatively regulated plant resistance to *Phytophthora*, whereas chloroplast-preferred MORF
138 proteins (NbMORF2b, NbMORF2c, and NbMORF9) positively regulated plant immunity.

139

140

141 **Results**

142 **Mitochondrion- and chloroplast-localized MORF proteins exert opposite immune functions**
143 **against *P. parasitica***

144 A VIGS-based approach was employed to identify negative regulators of plant resistance to
145 *P. parasitica*. This led to the identification of NbMORF8, an orthologue of AtMORF8 as
146 revealed by rigorous phylogenetic analysis, which is a MORF family protein. We also found that
147 the expression of multiple annotated *NbMORF* members was up-regulated in *N. benthamiana*
148 during *P. parasitica* infection as shown in our RNA-seq data (Jia, 2017). These results suggested
149 that *MORF* family genes may participate in the interaction between *P. parasitica* and *N.*
150 *benthamiana*. Hence, we decided to further explore the potential immune role of *NbMORF* genes
151 in *N. benthamiana*.

152 To characterize putative MORF members in *N. benthamiana*, we performed BLASTP
153 search against the predicted gene open reading frames of *N. benthamiana* using Arabidopsis
154 MORF proteins as queries to identify candidate *NbMORF* genes. Twenty candidate *NbMORF*
155 genes were obtained (Supplemental Table S1). We further cloned eight candidate genes, using
156 PCR amplification from cDNA libraries: *NbMORF1a*, *NbMORF1b*, *NbMORF2a*, *NbMORF2b*,
157 *NbMORF2c*, *NbMORF8a*, *NbMORF8b*, and *NbMORF9*. The genes were named according to the
158 Arabidopsis orthologues. *NbMORF8a* was the negative regulator that we identified using VIGS.
159 A phylogenetic tree was constructed. All NbMORF proteins contain a conserved MORF box
160 sequence of approximately 100 amino acid residues, like their Arabidopsis orthologues (Fig. 1
161 and Supplemental Fig. S1). However, NbMORF2a lacks an N-terminal amino acid sequence
162 preceding the MORF box. NbMORF8b is truncated from the C-terminal to within the MORF
163 box when compared to NbMORF8a (Fig. 1 and Supplemental Fig. S1).

164 To test the immune functions of these *NbMORF* genes, we performed VIGS assays on *N.*
165 *benthamiana* followed by *P. parasitica* inoculation. *NbMORF1a* and *NbMORF1b* or
166 *NbMORF2b* and *NbMORF2c* showed high sequence similarity, so we co-silenced
167 *NbMORF1a/1b* and *NbMORF2b/2c*, respectively (Supplemental Fig. S2). Leaves detached from
168 plants 14 d after inoculation with VIGS constructs were inoculated with *P. parasitica* zoospores.
169 The results showed that the *TRV-NbMORF2a* and *TRV-NbMORF9* plants exhibited bleached
170 leaves and were more susceptible to *P. parasitica* (Fig. 1 and Supplemental Fig. S2).
171 *TRV-NbMORF2b/2c* plants were more susceptible but did not exhibit any bleaching phenotype

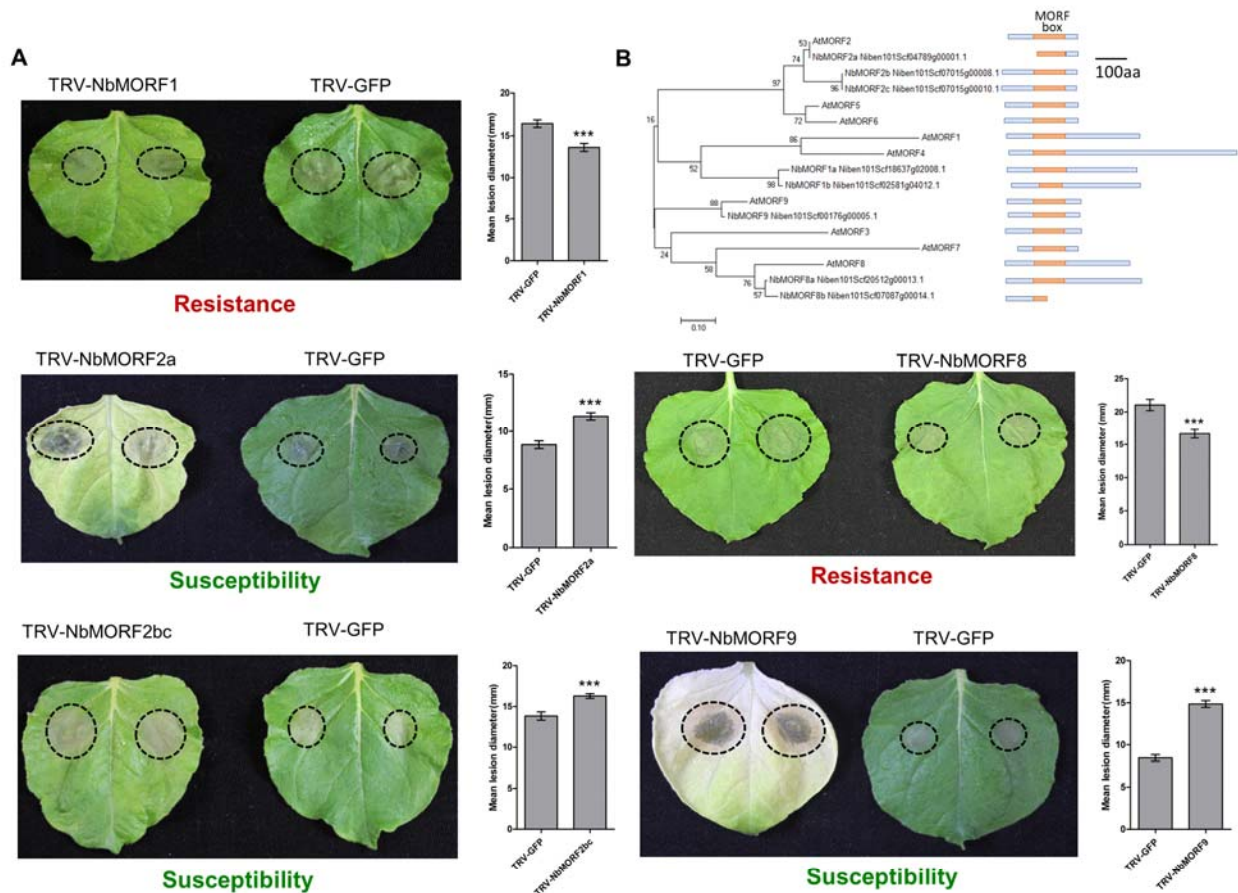


Figure 1. MORF proteins play different immune roles in *N. benthamiana* to *Phytophthora* pathogens. A, Silencing of *NbMORF1a/1b*, *NbMORF2a*, *NbMORF2b/c*, *NbMORF8* or *NbMORF9*, respectively, in *N. benthamiana* led to different responses to *P. parasitica*: silencing *NbMORF1a/1b* or *NbMORF8* enhanced resistance, while silencing of *NbMORF2a*, *NbMORF2b/c* or *NbMORF9* promoted *P. parasitica* colonization. Images were taken at ~40 h after inoculation with *P. parasitica* zoospore. Results were the mean \pm SE of 20 infections from at least 10 leaves. Statistical significance was assessed by *t* test. *** $P < 0.001$. Similar results were observed in three independent experiments. B, Cladogram of similarities between the AtMORF and NbMORF proteins. The phylogenetic tree was constructed by using the NJ method. All NbMORF proteins share a conserved MORF box.

172 (Fig. 1 and Supplemental Fig. S2). Silencing *NbMORF1a/1b* or *NbMORF8* enhanced resistance
 173 to pathogens and showed reduced plant height, malformed leaves and flowers, and infertility
 174 when the plants began forming flowers (Fig. 1, Supplemental Fig. S2, and Supplemental Fig.
 175 S3). Quantitation of gene expression confirmed that *NbMORF* genes in VIGS plants were at least
 176 80% reduced (Supplemental Fig. S2). As silencing of *NbMORF2a* or *NbMORF9* resulted in
 177 bleached leaves, we did not analyze them further. PTI and ETI are the two major layers of the
 178 plant immune system. To examine whether *NbMORF* genes participate PTI- or ETI-induced HR,
 179 we transiently expressed the *P. infestans* elicitor gene *INF1*, *Bax*, *P. infestans* RXLR effector
 180 genes, and cognate potato resistance genes *R3a/Avr3a^{KI}*, *RB/Avrblb1*, and *RpiVnt1/AvrVnt1*, in
 181 the *NbMORF*-silenced leaves. The results showed that *NbMORF1ab*- or *NbMORF2bc*-silenced
 182 leaves had no influence on HR (Supplemental Fig. S4). However, silencing *NbMORF8*

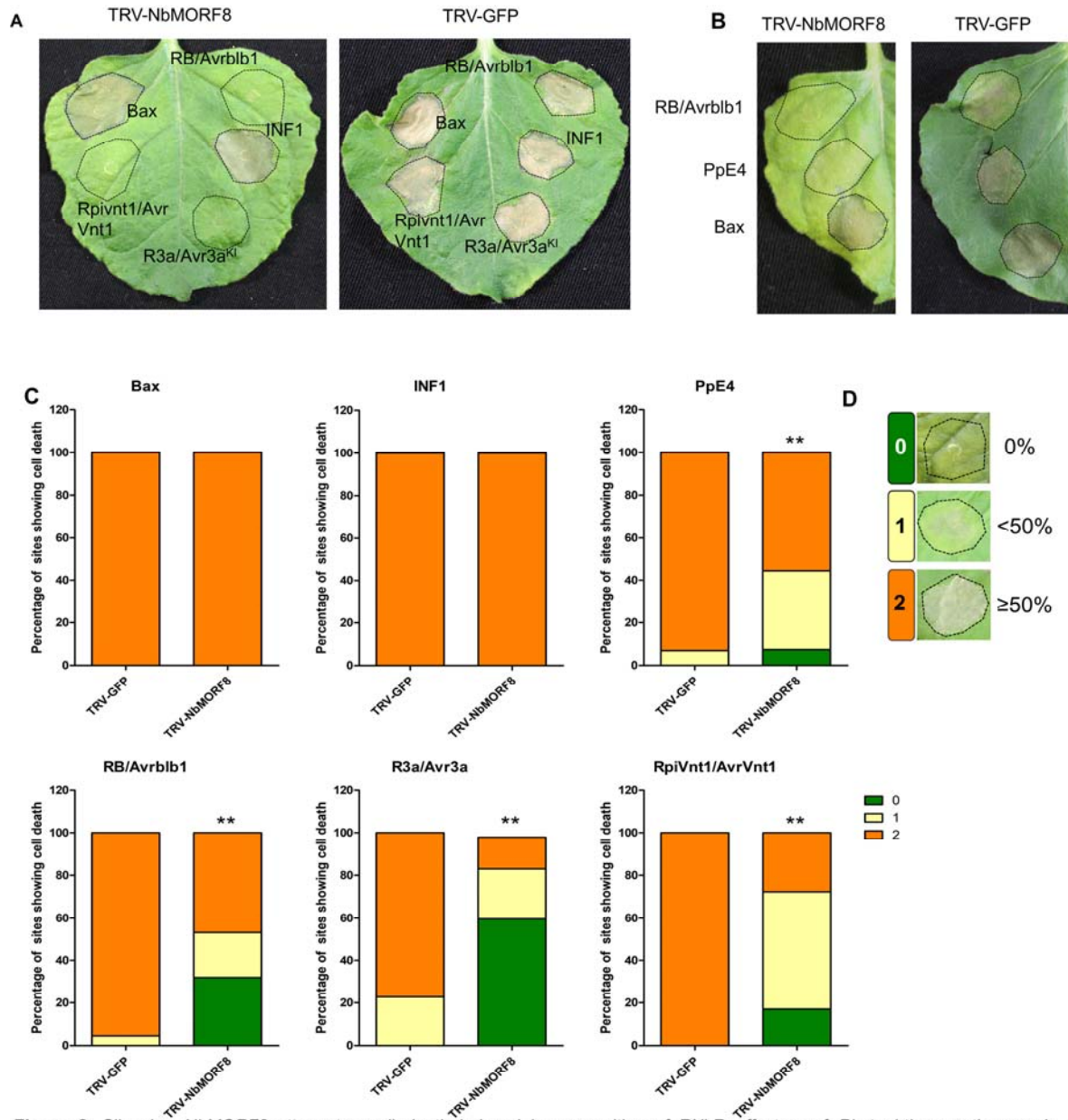


Figure 2. Silencing *NbMORF8* attenuates cell death induced by recognition of RXLR effectors of *Phytophthora* pathogens in *N. benthamiana*. A, Cell death observation of *NbMORF8*-silenced plants and control. Images were taken at five days after *A. tumefaciens*-mediated transient expression of *Avr/R* gene pairs, *INF1*, and *Bax* on VIGS plants. B, *NbMORF8*-silenced plants attenuated cell death induced by *P. parasitica* effector PpE4. C, The cell death severity assessment of the *NbMORF8*-silenced leaves and control leaves. Results were the mean \pm SE of at least 25 leaves from 10 plants for each group. Statistical significance was assessed by Wilcoxon-Mann-Whitney test. ** $P < 0.01$. Similar results were observed in at least six independent experiments. 0, no necrosis (green); 1, necrosis area <50% of the agroinfiltrated area (yellow); 2, necrosis area >50% of the agroinfiltrated area (orange). D, Quantitation of cell death. 0, no necrosis (green); 1, necrosis area <50% of the agroinfiltrated area (yellow); 2, necrosis area >50% of the agroinfiltrated area (orange).

183 suppressed HR induced by *R/Avr* recognition but not by INF1 or Bax (Fig. 2). These results
 184 suggest that *NbMORF8* participates in the ETI-induced HR response.

185 To further confirm the role of *NbMORF* genes in immunity, *NbMORF1a*, *NbMORF1b*,
 186 *NbMORF2b*, *NbMORF2c*, *NbMORF8a*, and *NbMORF8b* were over-expressed in *N.*
 187 *benthamiana* leaves followed by inoculation with *P. parasitica*. The results showed that

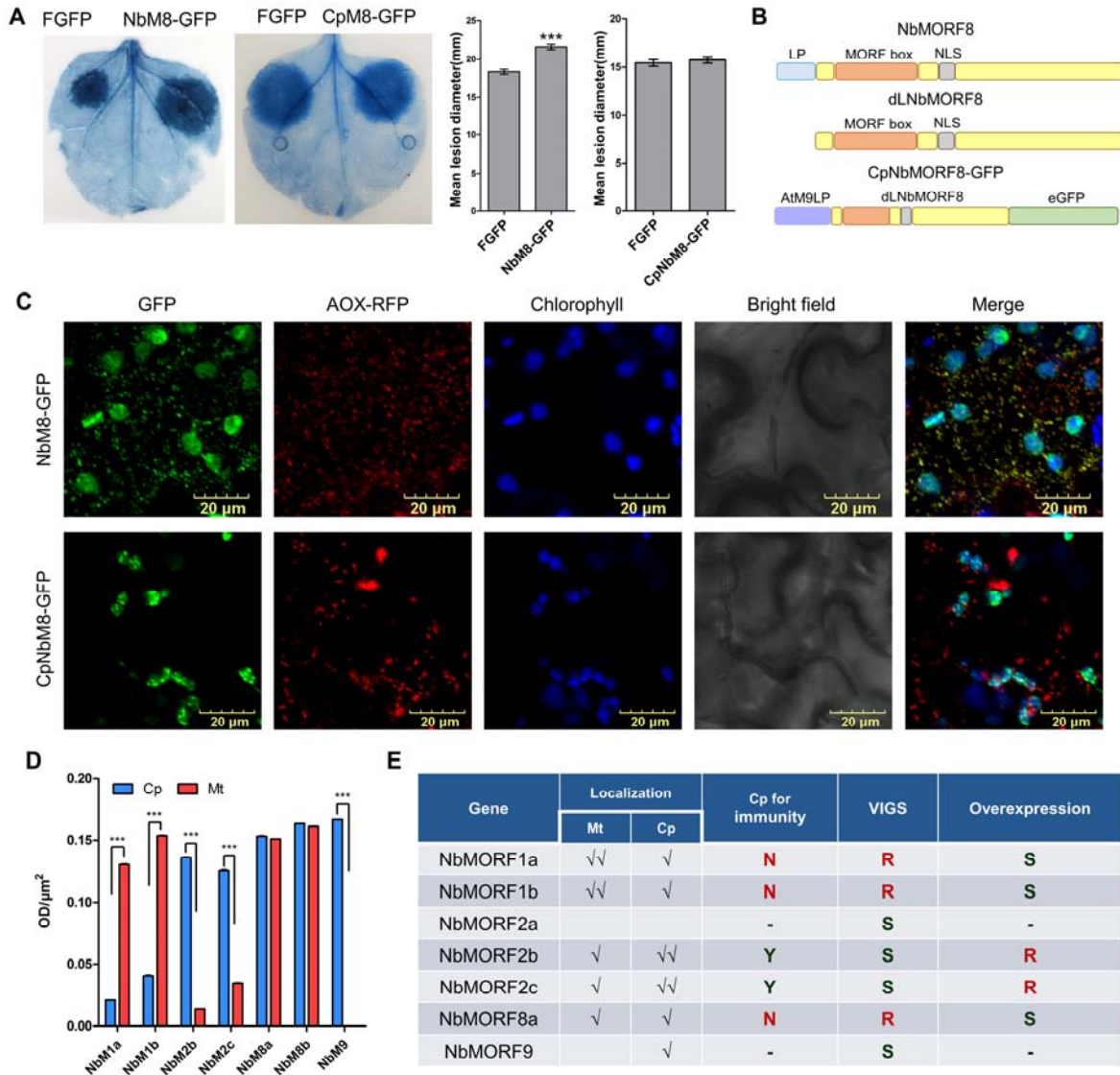


Figure 3. Mitochondrial and chloroplast localized MORF proteins exert opposing roles in the immune response to *Phytophthora* pathogens in *N. benthamiana*. **A**, *P. parasitica* inoculation assay on *CpNbMORF8* or *NbMORF8* overexpression leaves. Images were taken at 36 h after zoospore inoculation, with *GFP* plants used as a control. The inoculated leaves were stained with trypan blue to indicate the lesion area. Lesion diameter results were the mean \pm SE of 10 biological replicates. Similar results were observed in three independent experiments. Statistical significance was assessed by *t* test. *** $P < 0.001$. **B**, Schematic view of NbMORF8, dLNbMORF8, and CpNbMORF8. LP, leading peptide. NLS, nuclear localization signal. dL, deleting leading peptide. The leading peptide of NbMORF8 was replaced with the AtMORF9 leading peptide to re-target the fusion proteins to the chloroplast. The NbMORFs were analyzed using the same method. **C**, Subcellular localization of NbMORF8 and CpNbMORF8. Confocal microscopy of *N. benthamiana* leaves expressing *NbMORF8-GFP* or *CpNbMORF8-GFP*. Subcellular localization was observed at 2 or 3 days post agroinfiltration (dpi). AOX-RFP was used as a mitochondrial marker. Chloroplasts of *N. benthamiana* leaf cells were identified by their chlorophyll autofluorescence, shown in blue. **D**, Mean density analysis of mitochondria and chloroplasts in the subcellular localization images of NbMORF proteins. The three mitochondria or chloroplasts showing the strongest fluorescence were analyzed from each image of NbMORF proteins using ImageJ. Three images of each NbMORF were analyzed. Results were the mean \pm SE of nine organelles from three images. Statistical significance was assessed by *t* test. *** $P < 0.001$. **E**, Summary of subcellular localization and immune function of NbMORF proteins. \checkmark , NbMORF protein localized. $\checkmark\checkmark$, NbMORF protein preference. -, not determined. N, chloroplast localization is not required for immune function. Y, chloroplast localization is required for immune function. R, resistant to *P. parasitica*. S, susceptible to *P. parasitica*.

188 overexpression of *NbMORF1a*, *NbMORF1b*, or *NbMORF8a* enhanced plant susceptibility to *P.*
 189 *parasitica* (Fig. 3 and Supplemental Fig. S5), while overexpression of *NbMORF2b* or
 190 *NbMORF2c* led to increased resistance. Overexpression of *NbMORF8b* had no effect on plant

191 immunity (Supplemental Fig. S5). We also found that the transcript levels of *NbMORF1a*,
192 *NbMORF1b*, *NbMORF2a*, *NbMORF2b*, *NbMORF2c*, *NbMORF8a*, and *NbMORF9* were all
193 induced during infection (Supplemental Fig. S6: primers to distinguish *NbMORF2b* and *2c* could
194 not be designed because of the high sequence similarity). These results implied that *NbMORF*
195 genes, with the exception of *NbMORF8b*, are involved in plant immune response to
196 *Phytophthora* infection.

197 It was reported that all AtMORF family proteins are targeted to mitochondria or
198 chloroplasts (Bentolila et al., 2012; Takenaka et al., 2012). To examine whether NbMORF
199 proteins have similar subcellular localization as their Arabidopsis orthologues, we performed
200 transient expression of GFP-tagged NbMORF proteins in *N. benthamiana* and monitored
201 fluorescence using confocal microscopy. The localization of six NbMORF proteins
202 (*NbMORF1a*, *NbMORF1b*, *NbMORF2b*, *NbMORF2c*, *NbMORF8a*, and *NbMORF8b*) were
203 dually targeted to mitochondria and chloroplasts (Fig. 3 and Supplemental Fig. S7). *NbMORF9*
204 was detected only in chloroplasts (Supplemental Fig. S7). However, the mean density analysis,
205 which showed the fluorescence intensities of mitochondria and chloroplasts, indicated that
206 *NbMORF1a* and *NbMORF1b* were preferentially targeted to mitochondria, while *NbMORF2b*
207 and *NbMORF2c* were preferentially targeted to chloroplasts. *NbMORF8a* and *NbMORF8b* were
208 targeted to both mitochondria and chloroplasts without preferences (Fig. 3). *NbMORF2a*, which
209 lacked a leading peptide, was targeted to the cytoplasm and nucleus (Supplemental Fig. S7).

210 To determine whether localization of NbMORF proteins (*NbMORF1a*, *NbMORF1b*,
211 *NbMORF2b*, *NbMORF8a*, and *NbMORF2c*) to either plastids or plastids and mitochondria is
212 required for their immune functions, we targeted GFP-tagged NbMORF proteins to chloroplasts
213 (Cp-NbMORF) by replacing the NbMORF leading peptides with AtMORF9's leading peptide,
214 which is reported to target the protein to the chloroplast (Takenaka et al., 2012). *NbMORF2b* and
215 *NbMORF2c* only differ in the leading peptide. The results showed that the GFP-derived
216 fluorescence was detected exclusively in the chloroplasts (Fig. 3 and Supplemental Fig. S8). The
217 pathogen inoculation assay showed that the targeted chloroplast localization of *NbMORF1a*,
218 *NbMORF1b*, and *NbMORF8a* abolished their ability to enhance plant susceptibility
219 (Supplemental Fig. S9). However, *NbMORF2b/2c* still enhanced the resistance (Supplemental
220 Fig. S9). These results demonstrate that mitochondrial-preferred NbMORF members
221 (*NbMORF1a*, *NbMORF1b*) are negative regulators of host immunity, while

222 chloroplast-preferred NbMORF members (NbMORF2b, NbMORF2c, and NbMORF9) are
223 positive regulators. NbMORF8a, targeted to both organelles, functions in mitochondria and acts
224 as a negative regulator of plant immunity to *P. parasitica*.

225 ***NbMORF8* is a negative regulator of plant immunity to multiple *Phytophthora* pathogens**

226 As *NbMORF8* silencing not only showed enhanced resistance to *P. parasitica* but also
227 attenuated HR induced by ETI, we chose *NbMORF8* for further analysis. To examine whether
228 *NbMORF8* silencing conferred resistance to different *Phytophthora* pathogens, we also
229 inoculated *TRV-NbMORF8* leaves with *P. infestans* and *P. capsica* (Supplemental Fig. S10). The
230 results consistently showed that silencing *NbMORF8* conferred enhanced resistance to all tested
231 *Phytophthora* pathogens. Both the lesion diameter of these two pathogens and the sporulation of
232 *P. infestans* were significantly reduced (Supplemental Fig. S10).

233 While *NbMORF8*-silenced plants were morphologically indistinguishable from the
234 *TRV-GFP* control plants at the point of pathogen inoculation (Supplemental Fig. S3), they started
235 to show altered growth phenotypes, including reduced plant height, malformed leaves and
236 flowers, and infertility when progressing from vegetative growth to reproductive stages
237 (Supplemental Fig. S3), suggesting a role in plant development. *NbMORF8*-silenced plants
238 exhibited fewer flowers compared to the *TRV-GFP* control plants and most of these flowers had
239 deformed petals, with very few pollen particles and a shortened stigma, leading to sterility
240 (Supplemental Fig. S3).

241 **Silencing *NbMORF8* leads to enhanced ROS levels and up-regulated expression of** 242 **defense-related genes *NbPRI* and *NbPR2***

243 As mitochondria and chloroplasts are an important source of ROS (Amirsadeghi et al.,
244 2007; Colombatti et al., 2014) and NbMORF8 targets these two organelles, we examined ROS
245 levels in the *TRV-NbMORF8* plants using a luminol-based chemiluminescence assay. As shown
246 in Fig. 4, upon PAMP flg22 treatment, silencing *NbMORF8* resulted in higher ROS levels
247 compared to the *TRV-GFP* plants, suggesting that *NbMORF8* may regulate plant immunity
248 through regulation of ROS bursts. Interestingly, water treatment also induced ROS bursts in
249 *NbMORF8*-silenced plants after 10 min of treatment.

250 To further examine whether *NbMORF8* participates in the regulation of immune signaling
251 pathways, we tested the expression levels of PTI marker genes *NbWRKY7* and *NbWRKY8* (Yan
252 et al., 2016), SA pathway markers *NbPRI* and *NbPR2* (Yan et al., 2016), and JA pathway

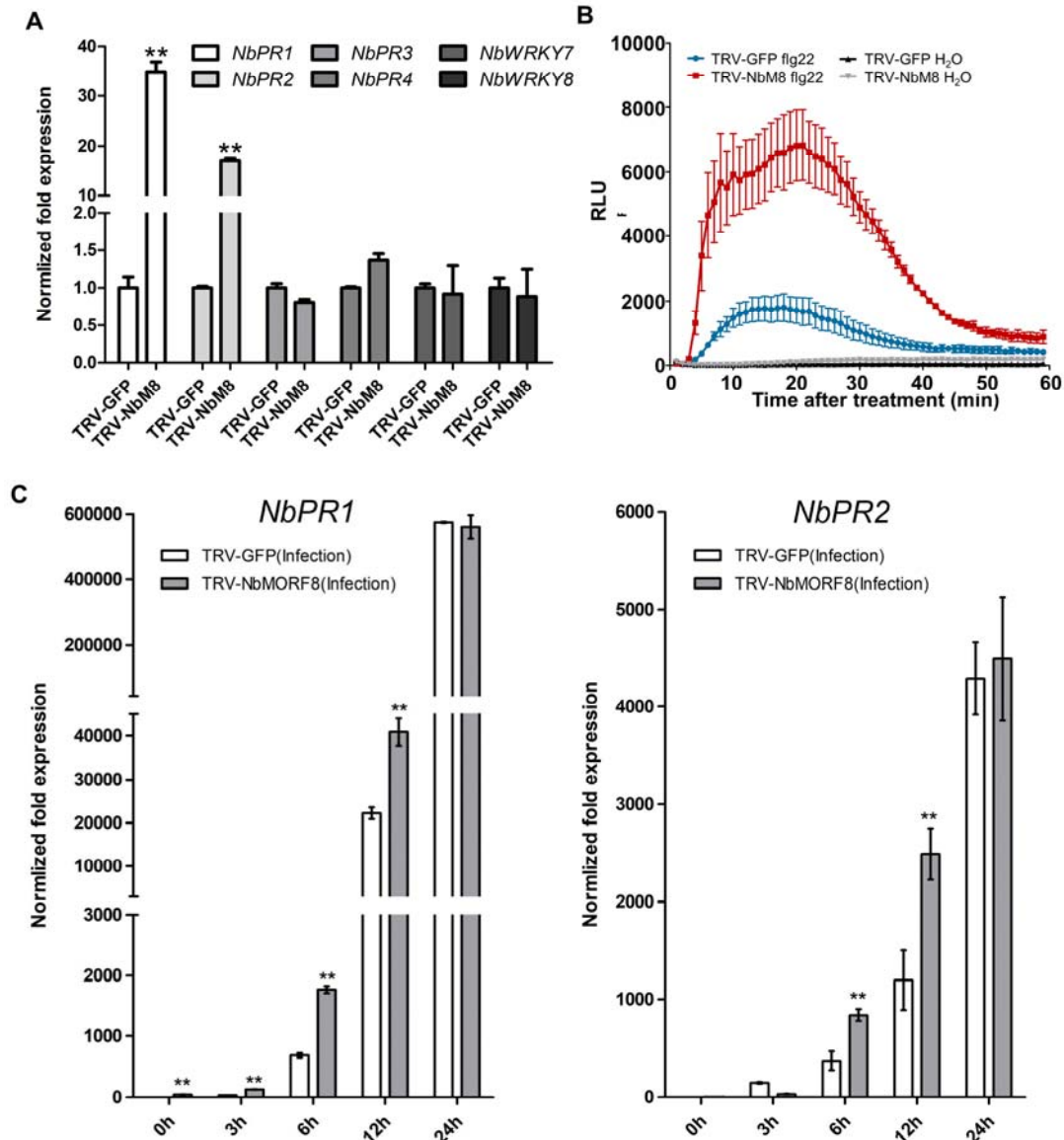


Figure 4. Silencing *NbMORF8* up-regulated expression of defense-related genes and enhanced ROS levels. A, Up-regulated expression of defense-related genes *NbPR1* and *NbPR2* in *TRV-NbMORF8* plants without pathogen treatment, as determined by RT-qPCR. B, ROS burst upon flg22 treatment of *NbMORF8*-silenced leaves. At least 12 leaves from six plants of each group were measured using a luminol-based chemiluminescence assay. C, The expression levels of *NbPR1* and *NbPR2* in *TRV-NbMORF8* plants in the early *P. parasitica* infection stage. Total RNA was extracted from *P. parasitica* zoospore-infected leaves at 3, 6, 12, and 24 h post inoculation (hpi). The *N. benthamiana EF1a* gene was used as an internal control. Results were the mean \pm SE. Similar results were observed in at least three independent experiments.

253 markers *NbPR3* and *NbPR4* (Yang et al., 2016) in *NbMORF8*-silenced plants. The results
 254 showed that silencing *NbMORF8* up-regulated *NbPR1* and *NbPR2* expression even without
 255 inoculation of *P. parasitica* (Fig. 4). We further detected the expression of *NbPR1* and *NbPR2*
 256 during early infection stage of *P. parasitica* on *TRV-NbMORF8* leaves. These results indicate
 257 that *NbMORF8* suppresses plant immunity by negatively regulating *NbPR1* and *NbPR2*
 258 expression and the SA signaling pathway (Fig. 4).

259 ***NbMORF8* is involved in C-to-U RNA editing of mitochondria and chloroplast genes**

260 As NbMORF proteins and their RNA editing sites in *N. benthamiana* are not certain, we
261 examined whether NbMORF8 functions in C-to-U RNA editing. DNA sequencing has been
262 widely used to identify RNA editing sites and measure editing levels in recent years (Zhu et al.,
263 2012; Hartel et al., 2013; Brehme et al., 2015; Shi et al., 2015; Yang et al., 2017; He et al., 2018;
264 Zhao et al., 2019). We amplified and sequenced orthologues of target genes shown to be edited
265 in *A. thaliana* by AtMORF8 (Bentolila et al., 2012; Bentolila et al., 2013; Glass et al., 2015)
266 from cDNA isolated from *TRV-GFP* and *TRV-NbMORF8* plants, respectively, and *N.*
267 *benthamiana* genomic DNA. The *NbMORF8*-silenced plants showed significant reductions in
268 the level of editing of mitochondrial genes *ccb206* (8 of 33 sites), which plays a role in
269 cytochrome c synthesis; *cob* (1 of 8 sites), which encodes a subunit of complex III; and
270 chloroplast gene *ndhB* (1 of 8 sites), which encodes a subunit of NADH dehydrogenase (Fig. 5).
271 However, editing of *ndhB*-242 was only slightly reduced. We further confirmed the defects in
272 editing of *cob*-853 and *ndhB*-242 using high-resolution melting analysis (HRM) (Supplemental
273 Fig. S11).

274 The *ccb206* protein is involved in synthesis of cytochrome c, which participates in electron
275 transport (Itani and Handa, 1998). Editing of *ccb206* transcripts in *TRV-NbMORF8* plants was
276 the most affected, and loss of editing was predicted to substantially change the *ccb206*
277 transmembrane structure (Fig. 5 and Supplemental Fig. S12), which suggests that silencing
278 *NbMORF8* may reduce cytochrome c levels. Furthermore, since *cob* encodes a subunit of
279 complex III in the mitochondrial electron transport chain (Weiss, 1987), loss of RNA editing
280 may cause defects in complex III function. We further examined the levels of cytochrome c and
281 complex III activities in both *TRV-NbMORF8* and *TRV-GFP* plants using ELISA. The results
282 showed that the cytochrome c level and complex III activities were significantly reduced in
283 *NbMORF8* -silenced plants (Fig. 5).

284 Editing of *ccb206* transcripts in *TRV-NbMORF8* plants was the most affected. Hence, we
285 also examined editing of *ccb206* transcripts during the early infection stage by *P. parasitica*,
286 during which the editing of two more sites, *ccb206*-367 and *ccb206*-380, were significantly
287 reduced in the *NbMORF8*-silenced plants (Fig. 5). In addition, the level of RNA editing of
288 *ccb206*-367 was about 80% without inoculation, but was further up-regulated in the *TRV-GFP*
289 plants when the plants were inoculated with *P. parasitica* (Fig. 5), suggesting that the RNA
290 editing of *ccb206* may also be regulated by *P. parasitica* infection.

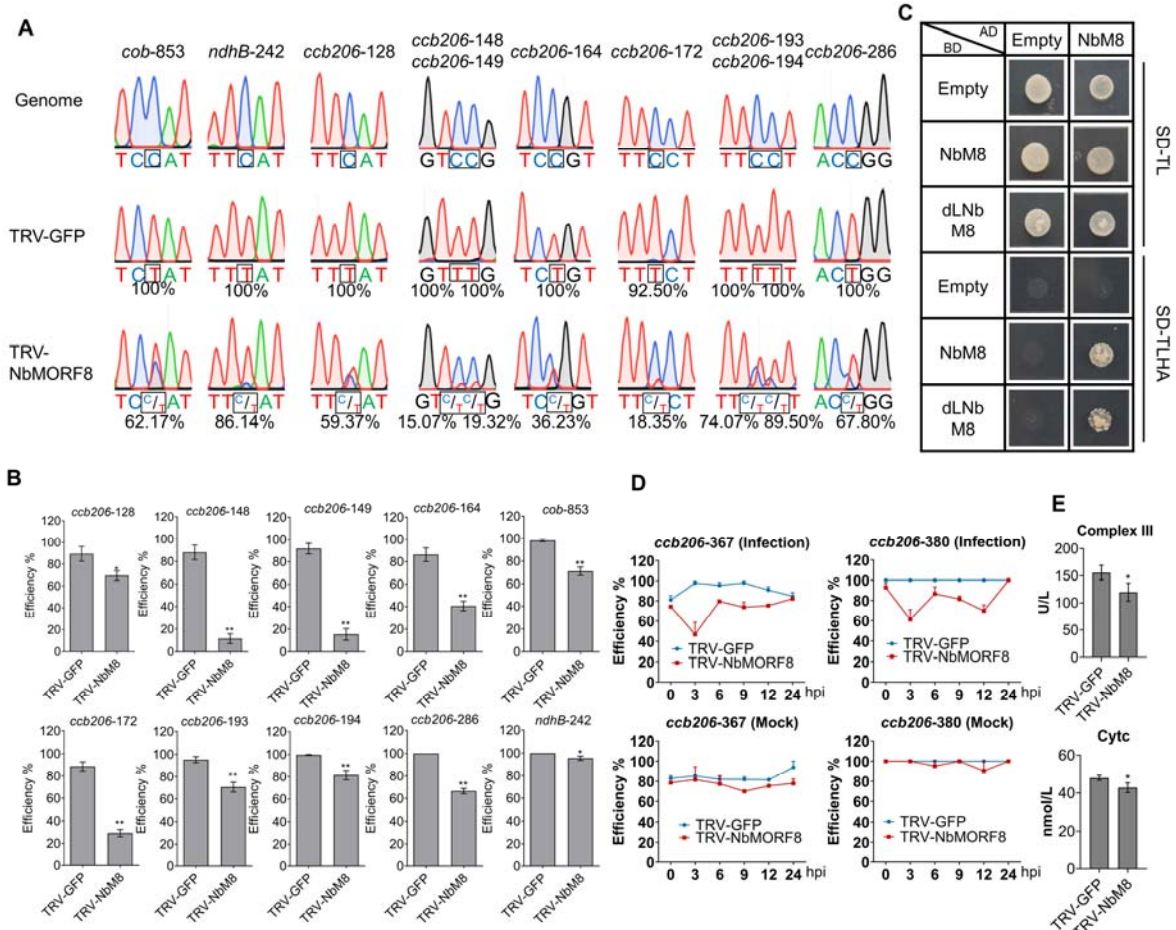


Figure 5. Silencing *NbMORF8* impaired RNA editing of *ccb206*, *cob*, and *ndhB*. A-B, The editing levels of mitochondrial *ccb206* transcripts at sites 128, 148, 149, 164, 172, 193, 194, and 286, and *cob* at site 853, and chloroplast *ndhB* at site 242. Results were the mean \pm SE of three biological replicates. Statistical significance was assessed by *t* test. * $P < 0.05$ ** $P < 0.01$. C, Yeast transformants were separately transferred onto SD-/Leu-/Trp (SD-LT) and SD-/Leu-/Trp-/His-/Ade (SD-LTHA) medium. The growth of yeast transformants on SD-LT medium demonstrated successful transformations. The growth of yeast transformants on SD-LTHA indicates interactions. Image was taken three days after dropping the transformed yeast on SD-/LTHA medium. D, The RNA editing of *ccb206* transcripts at sites 367 and 380 was down-regulated in *NbMORF8*-silenced plants during *P. parasitica* infection. Total RNA was extracted from *P. parasitica* zoospore-infected leaves of TRV- *NbMORF8* and TRV-*GFP* leaves at 3, 6, 12, 24, and 48 h post inoculation (hpi). Water was used as a control at each time point. Results were the mean \pm SE of three biological replicates. E, The cytochrome c levels and complex III activities were detected using ELISA. Results were the mean \pm SE of three biological replicates. Statistical significance was assessed by *t* test. * $P < 0.05$.

291 AtMORF8 was reported to form homomers (Zehrmann et al., 2015; Bayer-Csaszar et al.,
 292 2017). We used yeast-two-hybrid assay to examine whether NbMORF8 had a similar function,
 293 and confirmed that NbMORF8 could form homomers in yeast cells (Fig. 5), which indicated that
 294 NbMORF8 has a similar function to its *A. thaliana* orthologue *AtMORF8* and plays a role in
 295 C-to-U RNA editing.

296 **The MORF box of NbMORF8 is not required for its immune function**

297 The conserved MORF box is crucial for MORF protein interaction with PPRs and
 298 formation of heteromers or homomers. Moreover, it has distinct affinities to the PPR to regulate
 299 the RNA editing of different sites (Bayer-Csaszar et al., 2017; Haag et al., 2017). To analyze
 300 whether the immune function of NbMORF8 was dependent on its MORF box, we created a

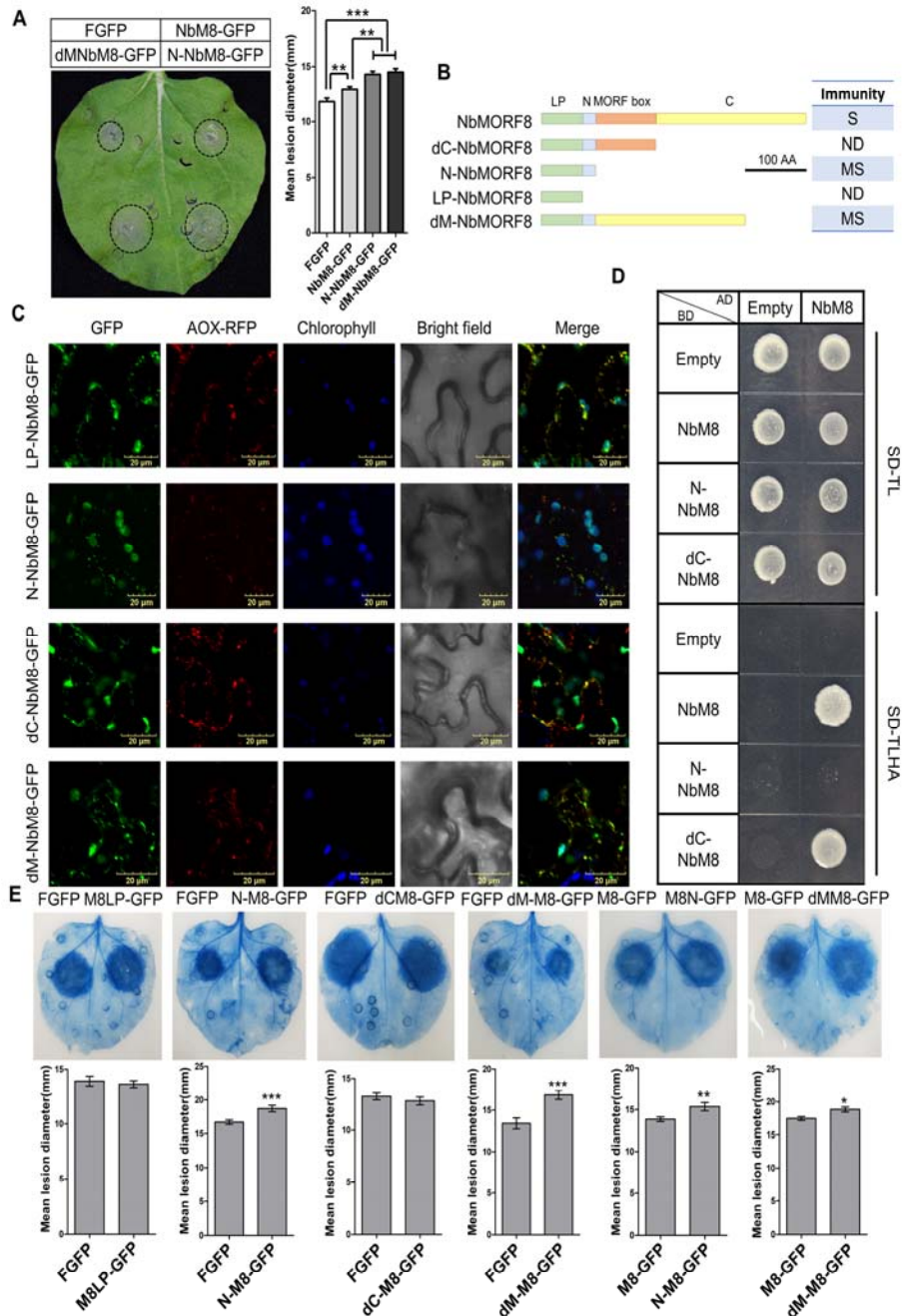


Figure 6. The MORF box domain suppresses the immune function of *NbMORF8*. **A**, Overexpression of *NbMORF8* mutants without the MORF box rendered plants more susceptible than the full-length *NbMORF8*. Transient expression of *N-NbM8-GFP*, *dM-NbM8-GFP*, *NbM8-GFP*, and *GFP* in single *N. benthamiana* leaves was done by agroinfiltration, followed by inoculation with *P. parasitica* zoospores. Images were taken at 40 h after zoospore inoculation. Results were the mean \pm SE of nine biological replicates. Similar results were obtained in at least three independent experiments. Statistical significance was assessed by *t* test. **B**, Schematic view of *NbMORF8* deletion mutant constructs. LP, leading peptide. N, N terminal ahead of MORF box. C, C terminal behind MORF box. dC, deleting C terminal behind MORF box. dM, deleting C terminal ahead of MORF box. S, susceptibility. ND, no difference compared with GFP. MS, more susceptible than the full length *NbMORF8*. **C**, Subcellular localization of LP-NbMORF8, N-NbMORF8, dC-NbMORF8, and dM-NbMORF8 was determined using confocal microscopy in *N. benthamiana* leaves three days after agroinfiltration (dpi). AOX-RFP was used as a mitochondrial marker. Chlorophyll fluorescence was used as chloroplast marker, shown in blue. **D**, The yeast-two-hybrid assay of *NbMORF8* mutations. Yeast transformants were separately transferred onto SD/Leu/-Trp (SD-LT) and SD/Leu/-Trp/His/-Ade (SD-LTHA) medium. The growth of yeast transformants on SD-LT medium demonstrated successful transformations, and the growth of yeast transformants on SD-LTHA medium indicated interactions. Images were taken five days after dropping the transformed yeast cells on SD-LTHA medium. **E**, The immune function of *NbMORF8* mutants was determined by transient overexpression in *N. benthamiana* followed by inoculation with *P. parasitica* zoospores. *GFP* was used as a control. The results of lesion diameter were the mean \pm SE of six biological replicates. Statistical significance was assessed by *t* test. * $P < 0.05$ ** $P < 0.01$ *** $P < 0.001$. Similar results were obtained in at least three independent experiments. Images were taken at 36 h after zoospore inoculation for *P. parasitica*. The inoculated leaves were stained with trypan blue to show the lesion area.

301 series of deletion mutant constructs (Fig. 6). All the mutant constructs preserved the leading

302 peptide to avoid altered localization. The localization of NbMORF8 deletion mutants were
303 monitored by transient expression of GFP-tagged versions in *N. benthamiana* followed by
304 confocal microscopy observation. All NbMORF8 mutant proteins were localized in
305 mitochondria and chloroplasts, like NbMORF8 (Fig. 6). Mutants were overexpressed in *N.*
306 *benthamiana* leaves, with *GFP* as a control, followed by inoculation with *P. parasitica*
307 zoospores. The results showed that overexpression of NbMORF8 mutants with the MORF box
308 deleted displayed higher levels of susceptibility to *P. parasitica* compared to the full-length
309 NbMORF8 (Fig. 6). Overexpression of the leading peptide of NbMORF8 and the mutant
310 dCNbMORF8 did not promote susceptibility to *P. parasitica* (Fig. 6).

311 We also found that NbMORF8 contains a nuclear localization sequence (NLS) as was
312 predicted by LOCALIZER (Sperschneider et al., 2017) (Fig. 1). To determine whether
313 NbMORF8 has an immune function outside mitochondria and chloroplasts, we generated a
314 construct with the leading peptide (dLNbMORF8) deleted and overexpressed it in *N.*
315 *benthamiana* using GFP as a control. This was followed by *P. parasitica* inoculation. The results
316 showed that GFP-tagged dLNbMORF8 was localized in the nucleus and cytoplasm and its
317 ability to increase susceptibility was abolished (Supplemental Fig. S13). These results suggest
318 that NbMORF8 exerts its immune function in mitochondria but not in the nucleus or cytoplasm.
319 We confirmed overexpression of all deletion mutants in *N. benthamiana* leaves (Supplemental
320 Fig. S14 and Fig. S15). These results suggest that the MORF box is not required for the immune
321 function of NbMORF8 and may instead suppress its immune function.

322 To examine the RNA editing activity of the NbMORF8 deletion mutants, we performed
323 sequencing to identify RNA editing in the overexpression plant leaves. The results showed that
324 overexpression of *NbMORF8* or full-length *NbMORF8* led to slightly decreased or no editing
325 (Supplemental Fig. S14). As MORF proteins can form homomers to function as RNA editing
326 factors, we analyzed the interaction between full-length NbMORF8 and the NbMORF8-N
327 deletion mutant, the shortest mutant which still had immune function, using yeast-two-hybrid.
328 The results showed that NbMORF8-N lost interaction with full-length NbMORF8 though it
329 retained its immune function (Fig. 6), suggesting that the immune function of *NbMORF8* does
330 not require the interaction activity.

331 **Silencing *NbMORF8* suppresses the accumulation of RXLR effectors**

332 We found that silencing *MORF8* attenuated HR induced by *R3a/Avr3a^{KI}*, *RB/Avrblb1*, and

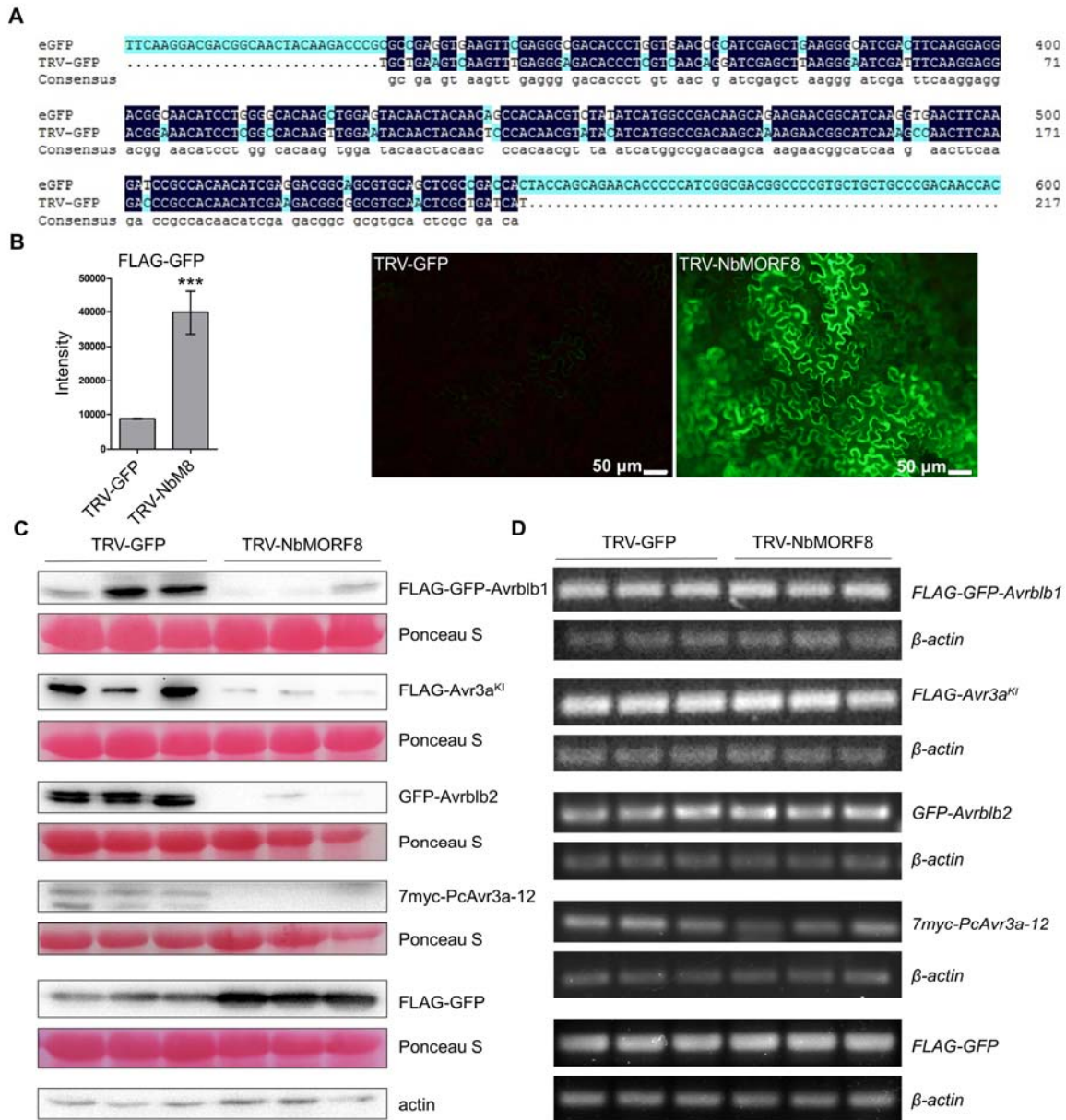


Figure 7. Silencing *NbMORF8* suppresses accumulation of *Phytophthora* effectors in *N. benthamiana*. **A**, Sequence alignment of eGFP and TRV-GFP fragments designed for silencing. **B**, Fluorescence intensity and eGFP accumulation in *NbMORF8*-silenced leaves. The eGFP fluorescence was detected at 4 dpi. For the fluorescence intensity analysis, six pictures from each group were analyzed using ImageJ. Results were the mean \pm SE of 6 pictures. Statistical significance was assessed by *t* test. *** $P < 0.001$. **C**, Western blot of the accumulation of RXLR effector proteins. Three lanes of each group indicate three biological replicates. Ponceau S staining shows equal loading of protein samples. **D**, Semi-quantitative PCR results of effector transcripts. Three lanes of each group show three biological replicates. *N. benthamiana* gene β -actin was used to normalize equal loadings.

333 *RpiVnt1/AvrVnt1* recognition, but not HR induced by INF1 or Bax (Fig. 2). We also tested *P.*
 334 *parasitica* RXLR effector PpE4 (Huang et al., 2019) in *TRV-NbMORF8* plants. Silencing
 335 *NbMORF8* consistently attenuated cell death induced by PpE4, which triggers cell death in *N.*
 336 *benthamiana* (Fig. 2). To test whether silencing *NbMORF8* affects efficiency of *Agrobacterium*
 337 *tumefaciens*-mediated transient expression, we examined protein accumulation of AVR3a^{KI} and

338 AVRblb1, whose HR was attenuated, and two more effectors (AVRblb2 and PcAVR3a12) that
339 do not trigger cell death on *NbMORF8*-silenced plant leaves, using GFP as a control. For all the
340 effectors examined, no differences were notable between transcript levels in *NbMORF8*-silenced
341 plants and the control (Fig. 7). However, the accumulation of RXLR effector proteins was
342 substantially decreased in *NbMORF8* -silenced plants (Fig. 7). Fluorescence intensities and GFP
343 accumulation levels were increased in *NbMORF8*-silenced leaves, which indicates that silencing
344 *NbMORF8* did not suppress *A. tumefaciens*-mediated transient expression (Fig. 7). Our results
345 suggest that *NbMORF8* is specifically required for the accumulation of *Phytophthora* RXLR
346 effectors.

347

348 **Discussion**

349

350 MORF family proteins are important RNA editing factors unique to land plants. To date,
351 most research on the MORF proteins has mainly focused on their interactions with RNA editing
352 factors (Hartel et al., 2013; Glass et al., 2015; Sun et al., 2015; Zehrmann et al., 2015;
353 Bayer-Csaszar et al., 2017; Hackett et al., 2017; Sandoval et al., 2019), or on their RNA editing
354 sites (Bentolila et al., 2012; Bentolila et al., 2013). However, the physiological processes
355 regulated by *NbMORF* genes are not well understood.

356 In this study, we identified that *NbMORF8* is a negative regulator of plant immunity to *P.*
357 *parasitica* and it functioned in mitochondria (Fig. 1, and Fig. 3). We confirmed that it is an RNA
358 editing factor in *N. benthamiana* (Fig. 5) by testing the editing extent of cytochrome c synthesis
359 related genes and the editing sites of AtMORF8-interacting PPR proteins. AtMORF8 is a crucial
360 editing factor in Arabidopsis and is involved in the RNA editing of 20% of chloroplast sites and
361 75% of mitochondrial sites, mainly in the editing of cytochrome c synthesis related genes
362 (Bentolila et al., 2012; Bentolila et al., 2013). RNA editing of *ccb206* in *TRV-NbMORF8* plants
363 was the most affected, and loss of editing was predicted to change the transmembrane structure
364 of the *ccb206* protein, which indicates silencing *NbMORF8* may significantly affect *ccb206*
365 function (Fig. 5 and Supplemental Fig. S12).

366 The *ccb206* protein is involved in the synthesis of cytochrome c, which participates in
367 electron transport (Itani and Handa, 1998). We further confirmed that cytochrome c levels were
368 decreased in *NbMORF8*-silenced plants (Fig. 5). We also found that editing of *ccb206* could be
369 regulated by *P. parasitica* in the early infection stage, and during which the editing of two more
370 sites, *ccb206-367* and *ccb206-380*, was significantly reduced in the *NbMORF8*-silenced plants
371 (Fig. 5). *NbMORF8* also participates in RNA editing of the *cob* gene, which encodes a
372 component of complex III in the respiratory electron transport chain (Weiss, 1987). These results
373 suggest that silencing *NbMORF8* may affect the respiratory electron transport chain, an
374 important source of ROS (Møller, 2001). Therefore, the *NbMORF8*-regulated ROS burst (Fig. 4)
375 is likely achieved through its effect on the functionality of respiratory chain components (Fig. 8).
376 However, there have been no reports on the role of *ccb206* or *cob* in the regulation of ROS/SA or
377 whether their RNA editing will have influence on ROS/SA. Future studies should focus on the
378 sites of ROS production in *NbMORF8*-silenced leaves to further analyze whether the high-level
379 ROS was produced in mitochondria or chloroplasts. *NbMORF8* also has a slight influence on
380 RNA editing of the *ndhB* gene, the Arabidopsis orthologue of which was reported to be involved

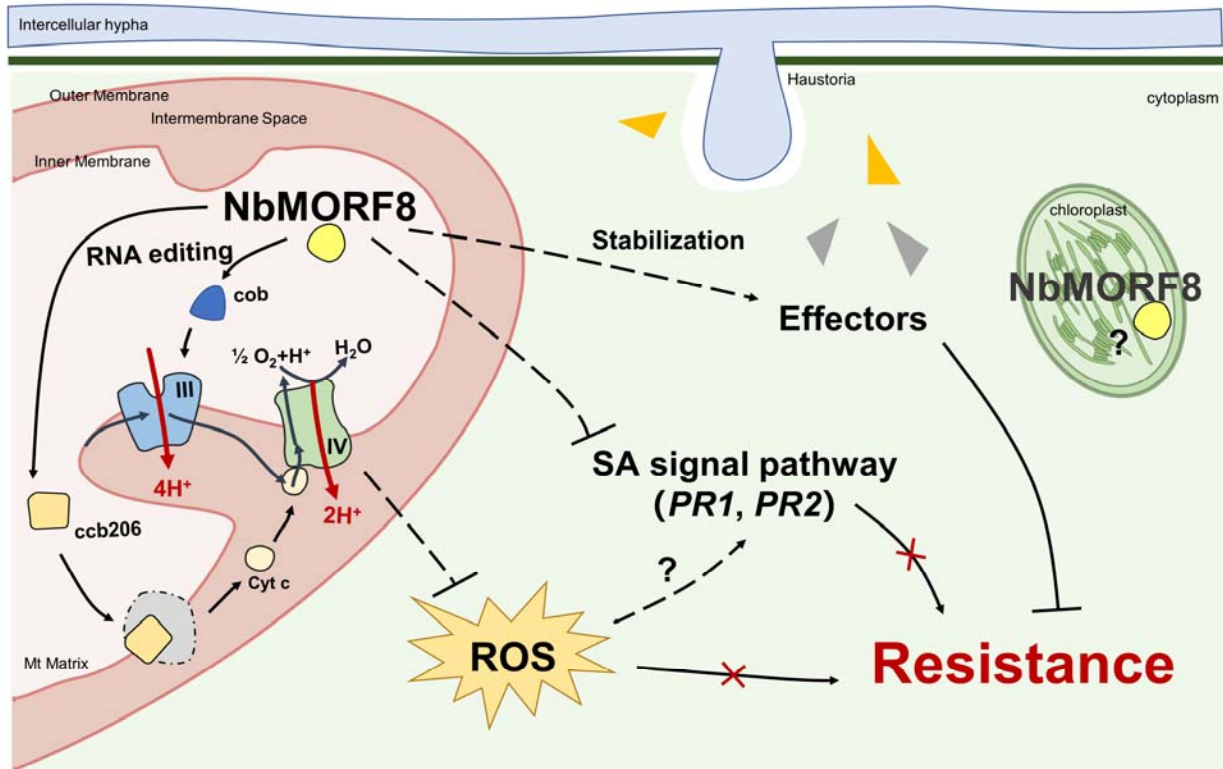


Figure 8. Schematic model for the role of NbMORF8 in plant immunity. NbMORF8 takes part in the RNA editing of mitochondrial *cob* and *ccb206* genes and further influence the levels of cytochrome c and complex III activity. Silencing of *NbMORF8* up-regulated the expression of SA signal pathway markers (*NbPR1* and *NbPR2*) and ROS level, which enhanced the immunity to *Phytophthora* pathogens. *NbMORF8* regulated ROS burst is likely achieved through its effect in functionality of respiratory chain components. But the ROS production sites in *NbMORF8* silenced leaves should be further analyzed to confirm whether the high-level ROS was produced in mitochondria or chloroplasts. *NbMORF8* are also required for the accumulation of *Phytophthora* RXLR effectors which will suppress the plant immunity. We have found that the mitochondrial localization of NbMORF8 is sufficient for its immune function. Whether the chloroplast localization takes part in plant immunity or whether it has influence in the cross-talk between mitochondria and chloroplasts need to be analyzed in the future.

381 in immunity (Garcia-Andrade et al., 2013).

382 The MORF box of MORF proteins has been revealed to mainly interact with PPR proteins
 383 (Bayer-Csaszar et al., 2017). The crystal structures of AtMORF1/AtRIP8 and AtMORF9/AtRIP9
 384 indicate that the interaction between MORF proteins occurs within the MORF box (Haag et al.,
 385 2017). Our results showed that both overexpression or silencing of *NbMORF8* resulted in
 386 suppression of RNA editing in some sites (Fig. 5 Supplemental Fig. S14), consistent with reports
 387 that both *AtMORF8* overexpression and silenced plants showed a negative effect on C-to-U RNA
 388 editing (Bentolila et al., 2012). These results suggest that NbMORF8 interacts with different
 389 RNA editing factors and alters the NbMORF8-dependent editosome, whether *NbMORF8* is
 390 silenced or overexpressed. Unexpectedly, the RNA editing level of all the overexpressed

391 *NbMORF8* deletion mutants decreased or showed no changes compared to the control, like that
392 of full-length *NbMORF8*, though the MORF box is known to be essential for the interaction
393 between MORF proteins and other RNA editing factors (Supplemental Fig. S14). It is possible
394 that the overexpression of *NbMORF8* mutants interfered with the endogenous *NbMORF8*
395 function.

396 Our results showed that the mutant NbMORF8-N lost its ability to interact with full-length
397 NbMORF8 but retained its immune function, even rendering plants more susceptible than
398 *NbMORF8* (Fig. 6), suggesting that the immune function of *NbMORF8* does not require the
399 interaction activity and the MORF box is likely suppressive to its immune function. Furthermore,
400 our results on the deletion mutant analysis of NbMORF1a, NbMORF2b, NbMORF2c, and
401 NbMORF8b showed that the N terminal region prior to the MORF box of these NbMORF
402 proteins was sufficient for their immune function (Supplemental Fig. S16), suggesting that
403 *NbMORF* genes may regulate plant immunity in a similar way. Considering that full-length
404 NbMORF8b is longer than NbMORF8b-N (containing ~40 amino acid residues of the
405 N-terminal MORF box) and NbMORF8b exhibited no immune function, it is likely that the
406 N-terminal MORF box suppresses the immune function of NbMORF8 (Supplemental Fig. S16).
407 Future studies should focus on identifying the interacting proteins of NbMORF8-N to investigate
408 how such a short region can function as an immune regulator.

409 Our results showed that silencing *NbMORF8* suppresses the HR triggered by avirulence
410 RXLR effectors, but has no influence on INF- or Bax-induced cell death (Fig. 2). In addition,
411 silencing *NbMORF8* enhanced disease resistance, possibly by activating the SA signaling
412 pathway (Fig. 4). We further showed that silencing *NbMORF8* specifically reduced
413 accumulation of multiple RXLR effectors of *Phytophthora* pathogens, but not their transcript
414 accumulation, since the accumulation of the control protein GFP was increased in
415 *NbMORF8*-silenced plants, which indicates that *NbMORF8* did not suppress
416 *Agrobacterium*-mediated transient expression (Fig. 7). Silencing *NbMORF8* and *NbMORF1a/1b*
417 showed some similar phenotypes: enhanced resistance to *P. parasitica*, higher ROS burst after
418 flg22 treatment, functioning in mitochondria, reduced plant height, curly leaves, and infertility
419 (Fig. 1, Fig. 4, Supplemental Fig. S2, Supplemental Fig. S3, and Supplemental Fig. S17). Our
420 further testing on PTI- and ETI-induced cell death showed that silencing *NbMORF1a/1b* had no
421 influence on cell death induced by recognition of RXLR effectors Avr3a^{K1}, Avrblb1, and

422 AvrVnt1 (Supplemental Fig. S4), suggesting that *NbMORF8* is the NbMORF member that is
423 specifically involved in accumulation of *Phytophthora* RXLR effectors.

424 We identified eight MORF family members in *N. benthamiana* and used VIGS assay
425 followed by *P. parasitica* inoculation to investigate their roles in plant immunity. Although
426 NbMORF2a has no leading peptide, the *NbMORF2a*-silenced plants exhibited bleached leaves
427 and were more susceptible to *P. parasitica* (Fig. 1 and Supplemental Fig. S2). Sequence
428 alignment showed that the predicted translated 5' UTR of *NbMORF2a* was identical to the
429 N-terminal MORF box of NbMORF2b and 2c (Supplemental Fig. S18), which indicates that the
430 predicted open reading frame of NbMORF2a may have lost its 5' sequence. Loss of C-to-U RNA
431 editing in mitochondria or chloroplasts usually leads to a defective phenotype, which is usually
432 manifested through bleached leaves, infertility, etc. (Takenaka et al., 2013; Barkan and Small,
433 2014). Most *NbMORF*-silenced plants showed significant phenotypic changes such as bleached
434 leaves (*NbMORF2a* and *NbMORF9*), reduced plant heights, malformed leaves and flowers, and
435 infertility (*NbMORF1a/1b* and *NbMORF8*), which are similar with their *A. thaliana* orthologues
436 (Takenaka et al., 2012). We further examined the immune signaling pathway that *NbMORF*
437 genes participate in using RT-qPCR assay. The results showed that *NbMORF1a/1b*-silenced
438 plants displayed up-regulated expression of *NbPRI*, *NbPR4*, and *NbWRKY7* (Supplemental Fig.
439 S17), while silencing *NbMORF2b/2c* down-regulated expression of *NbPRI*, *NbPR2*, *NbPR3*, and
440 *NbPR4* (Supplemental Fig. S17). Silencing *NbMORF8* up-regulated *NbPRI* and *NbPR2* (Fig. 4).
441 These results suggest that different NbMORF proteins are involved in regulating different signal
442 pathways.

443 Since mitochondria and chloroplasts are important source of ROS (Amirsadeghi et al.,
444 2007; Colombatti et al., 2014) and NbMORF proteins are targeted to these two organelles, we
445 examined ROS levels in the *TRV-NbMORF* plants. Silencing *NbMORF1a/b* or *NbMORF8*
446 resulted in higher ROS levels compared to the *TRV-GFP* plants, while silencing *NbMORF2b/c*
447 did not produce significant changes in maximum ROS burst. However, the ROS decreased faster
448 in *NbMORF2b/2c*-silenced plants (Supplemental Fig. S17). These results suggest that ROS may
449 play important roles in *NbMORF*-regulated immunity.

450 In summary, we found that *NbMORF8* negatively regulates plant immunity to *P. parasitica*
451 via mitochondrial targeting of its encoded protein and this function is independent of its MORF
452 box. The enhanced disease resistance of *NbMORF8*-silenced plants resulted from reduced

453 accumulation of effector proteins, activated SA signaling pathway, and enhanced ROS burst
454 (Fig. 8). Our work showed that the NbMORF family genes are involved in regulating plant
455 immune responses to *Phytophthora* pathogens, and the NbMORF members that are preferentially
456 targeted to mitochondria negatively regulate plant resistance against *Phytophthora*, whereas
457 NbMORF members that are preferentially targeted to chloroplasts are positive immune
458 regulators.

459

460 **Material and Methods**

461 **Plasmid constructs**

462 For VIGS, ~300bp specific fragments of *NbMORF* genes were chosen by the VIGS tool
463 (<http://vigs.solgenomics.net/>) and amplified from *Nicotiana benthamiana* cDNA. The fragment
464 of *NbMORF8* was cloned into pTRV2 vector between Xba1 and BamH1 sites while other
465 NbMORF family genes were between EcoR1 and Xho1 sites. For yeast-two-hybrid the resultant
466 products were cloned into pGBKT7 using the Nde1 and Xho1 sites and cloned into pGADT7
467 using EcoR1 and Xho1. *NbMORF8* and deletion mutants were amplified from *N. benthamiana*
468 cDNA and the leading peptide of *NbMORF8* was predicted using Mitoprot (Claros and Vincens,
469 1996) (<https://ihg.gsf.de/ihg/mitoprot.html>). The signal defining mitochondria or chloroplast
470 subcellular localization is contained within the first 100 amino acids (leading sequence) of a
471 protein's N terminus (Clark et al., 2009; Koprivova et al., 2010; Narsai et al., 2011). Hence, we
472 fused the first ~100 amino acids of NbMORFs to the N terminus of GFP (Bottin et al., 1999) to
473 detect the subcellular localization. To generate NbMORFs-eGFP fusion constructs, the fusion
474 fragments were amplified using overlap PCR and cloned into the pKannibal (Wesley et al., 2001)
475 vector using Xho1 and Xba1 sites. Then, the constructs were digested by Not1 and inserted into
476 pART27 (Gleave, 1992). All primers used are listed in Supplemental Table S2.

477 **Agroinfiltration and VIGS**

478 *Agrobacterium tumefaciens* strain GV3101 containing plasmid constructs was grown for 36
479 hours in LB medium with appropriate antibiotics at 28°C. The medium containing bacteria was
480 gathered and resuspended in infiltration buffer (10mM MES, 10mM MgCl₂ and 200 mM
481 acetosyringone) and adjusted to the required OD₆₀₀ before infiltration into *N. benthamiana* leaves
482 (the OD₆₀₀ was generally 0.3 for transient expression).

483 VIGS was performed as described previously (Senthil-Kumar and Mysore, 2014). Briefly,

484 *Agrobacterium* strains harboring the pTRV1 vector and pTRV2-GFP or pTRV2-NbMORFs were
485 mixed in a 1:1 ratio and the final OD₆₀₀ for each strain was 0.25. The co-cultures were then
486 infiltrated into the two largest leaves of 4-week old plants. Plants were grown for 2 more weeks
487 before using for *Phytophthora* infection or cell death assay. Plant growing conditions for *N.*
488 *benthamiana* were the same as previously described (Pan et al., 2016).

489 In the cell death assay, *A. tumefaciens* strain AGL1 was used for *RpiVnt1* and *AvrVnt1*
490 expression. The extent of cell death or HR was monitored daily up to 5 days
491 post-agroinfiltration. The extent of cell death or HR was divided into 3 categories: grade 0 - no
492 cell death of the agroinfiltrated area; grade 1 - clear necrosis occupying <50% of the
493 agroinfiltrated area; and grade 2 - necrosis area occupying >50% of the agroinfiltrated area.

494 **Confocal microscopy**

495 *N. benthamiana* cells expressing fusion proteins were observed two or three days after
496 infiltration using an Olympus FV3000 confocal microscope (Japan). RFP (GenBank:
497 ABC69141) was imaged using an excitation wavelength of 559 nm with emissions collected at
498 600-680 nm. GFP was excited at 488 nm with emissions collected at 500-540 nm. AOX-RFP
499 (Narsai et al., 2011) was used as the mitochondria fluorescent marker. Chloroplasts were
500 identified by their chlorophyll autofluorescence.

501 ***Phytophthora* infection assay**

502 *P. parasitica* strain Pp016, *P. capsici* strain LT263, and *P. infestans* strain 88069 were used
503 for plant infection. *P. parasitica*, *P. capsici*, and *P. infestans* culture and inoculation were
504 performed as in previous reports (Wang et al., 2011; Wang et al., 2013; Li et al., 2019). Zoospore
505 inoculation was performed by inoculating 2000 zoospores for *P. parasitica*, 800 for *P. capsici*
506 and 1200 for *P. infestans*. *P. infestans* sporangia counts were performed as described previously
507 on 10 days post inoculation leaves (McLellan et al., 2013; Boevink et al., 2016).

508 **Gene expression assay**

509 Total RNA was extracted using TRIzol reagent (Invitrogen). 800 ng total RNA was
510 reverse-transcribed into cDNA using a PrimeScript RT Reagent Kit with gDNA Eraser (Perfect
511 Real Time) (TaKaRa). Reverse transcription quantitative PCR (RT-qPCR) was performed using
512 FastStart Universal SYBR Green Master (ROX) (Roche) with specific primers in an iQ7
513 Real-Time Cycler (Life Technologies, USA). The relative gene expression level was calculated
514 using the $2^{-\Delta\Delta C_t}$ method with the housekeeping gene *Ppactin* as the reference for *P. parasitica*

515 and *EF1 α* or *β -actin* for *N. benthamiana*. Semi-quantitative PCR was performed using EasyTaq
516 DNA polymerase (TransGen Biotech) and amplified for 27 cycles. All primers are listed in
517 Supplemental Table S2.

518 **Yeast-two-hybrid assay**

519 The yeast-two-hybrid assay was performed as described in the Matchmaker Two-Hybrid
520 System 3 protocol (Clontech). The constructs of *NbMORF8* and its deletion mutants were
521 co-transformed into *Saccharomyces cerevisiae* strain AH109. The transformations were
522 confirmed by selection on SD/-Trp-Leu medium and the interaction was tested by selection on
523 SD/-Trp-Leu-His-Ade medium.

524 **RNA editing assay**

525 To analyze the extent of RNA editing, RNA was isolated from VIGS-treated plant leaves
526 and reverse transcribed into cDNA. The mitochondria and chloroplast genes were amplified with
527 specific primers and then sequenced. At the RNA editing sites, cDNA sequences were evaluated
528 for their respective C to T differences. The extent of RNA editing was estimated by the relative
529 height of the respective nucleotide peaks in the sequence analysis.

530 **Protein extraction and immunoblotting**

531 All the protein samples were extracted using GTEN buffer (10% v/v glycerol, 25mM
532 Tris-HCl (pH 7.5), 1 mM EDTA, 150 mM NaCl, 0.1% v/v Tween 20) with 10 mM DTT,
533 protease inhibitor cocktail and 0.1% (v/v) Nonidet P-40. Proteins were separated by sodium
534 dodecyl sulphate-polyacrylamide gel electrophoresis (SDS- PAGE). Gels were blotted onto
535 PVDF membranes (Roche) for 1.75 h at 250 mA in transfer buffer (25 mM Tris, 200 mM
536 glycine, 20% v/v methanol) and the membranes were blocked in 10% (w/v) skim milk in TBST
537 buffer (1 mM Tris, 0.15 M NaCl, 0.05% v/v Tween 20, pH 7.2) for 3-5 hours. The blocked
538 membranes were incubated with primary antibodies at 1:2000 dilution, either a monoclonal GFP
539 antibody raised in mouse (ABclonal, #AE012) or a monoclonal anti-FLAG antibody raised in
540 mouse (ABclonal, #AE005). The membranes were washed with TBST three times before
541 addition of the secondary antibody at 1:2000 dilution: HRP Goat Anti-Mouse IgG (H+L)
542 Antibody (ABclonal, #AS003). Before ECL (ComWin, #CW0049S) photographing using a
543 molecular imager (Bio-Rad, ChemiDocTM XRS+), the membranes were washed twice with
544 TBST buffer and once in TBS buffer (1 mM Tris, 0.15 M NaCl, pH 7.2).

545 **Bioinformatics**

546 For phylogenetic analysis, protein sequences of the AtMORF/RIP family were downloaded
547 from the Arabidopsis Information Resource (<http://www.arabidopsis.org/>). BLASTP searches
548 were then performed using AtMORF/RIP family protein sequences as queries with an expected
549 value (e-value) cutoff of e^{-10} using the Sol Genomic network
550 (<https://solgenomics.net/tools/blast/>) to identify the potential NbMORF/RIP family member
551 protein sequences. Alignment and phylogenetic analysis were performed using MEGA7 with
552 default parameters (Saitou and Nei, 1987; Kumar et al., 2016). The neighbor-joining method
553 with 1000 bootstrap replicates was used. The subcellular location of NbMORFs was predicted
554 using TargetP (Emanuelsson et al., 2000) and LOCALIZER (Sperschneider et al., 2017).

555 **ROS burst detection**

556 ROS production was measured with a previously reported luminol-based assay (Sang and
557 Macho, 2017). Two-week-silenced *N. benthamiana* leaves were sliced into 0.785 cm² leaf discs
558 and floated in water overnight. Water was replaced with reagent containing luminol, peroxidase,
559 and 1 μ M flg22. ROS released by leaf discs was detected by luminescence of luminol.

560 **High-resolution melting (HRM) analysis**

561 HRM assay was performed according to the method previously reported (Chateigner-Boutin
562 and Small, 2007). The PCR cycling and HRM were performed on a LightCycler 480 II machine
563 (Roche) and the HRM analysis was performed using Gene scanning software (Roche).

564 **Accession numbers**

565 Genes described here in have the following Sol Genomics Network (<https://solgenomics.net/>)
566 gene accession numbers: *NbMORF1a* (Niben101Scf18637g02008.1), *NbMORF1b*
567 (Niben101Scf02581g04012.1), *NbMORF2a* (Niben101Scf04789g00001.1), *NbMORF2b*
568 (Niben101Scf07015g00008.1), *NbMORF2c* (Niben101Scf07015g00010.1), *NbMORF8a*
569 (Niben101Scf20512g00013.1), *NbMORF8b* (Niben101Scf07087g00014.1), *NbMORF9*
570 (Niben101Scf00176g00005.1)

571 572 **Supplemental Data**

573 **Supplemental Figure S1.** Sequence alignment of all NbMORF and AtMORF proteins.

574 **Supplemental Figure S2.** Efficient silencing of *NbMORF* genes in *N. benthamiana*.

575 **Supplemental Figure S3.** *NbMORF8* is required for flower development in *N. benthamiana*.

576 **Supplemental Figure S4.** Silencing *NbMORF1a/1b* or *NbMORF2b/2c* had no influence on PTI

577 and ETI induced cell death.

578 **Supplemental Figure S5.** Multiple *NbMORF* genes are involved in immunity in *N. benthamiana*
579 to *P. parasitica*.

580 **Supplemental Figure S6.** The expression of *NbMORF* genes during *P. parasitica* infection.

581 **Supplemental Figure S7.** Subcellular localization of NbMORF proteins.

582 **Supplemental Figure S8.** Confocal microscopy of *N. benthamiana* leaf pavement cells
583 expressing CpNbMORF proteins.

584 **Supplemental Figure S9.** The effect of targeted expression of NbMORF proteins on their
585 immune functions.

586 **Supplemental Figure S10.** *NbMORF8*-silenced plants exhibited enhanced resistance to *P.*
587 *infestans* and *P. capsici*.

588 **Supplemental Figure S11.** The high-resolution melting (HRM) results of *cob-853* and
589 *ndhB-217, 242*.

590 **Supplemental Figure S12.** Prediction of transmembrane structure of the *ccb206*-encoded
591 protein.

592 **Supplemental Figure S13.** Overexpression of dLNbMORF8 did not promote *P. parasitica*
593 infection.

594 **Supplemental Figure S14.** RNA editing levels of different *NbMORF8* deletion mutants in *N.*
595 *benthamiana*.

596 **Supplemental Figure S15.** Detection of transiently-expressed NbMORF8 proteins and
597 NbMORF8 deletion mutant proteins in *N. benthamiana*.

598 **Supplemental Figure S16.** The role of the conserved MORF box of NbMORF proteins in their
599 immune function in *N. benthamiana* to *P. parasitica*.

600 **Supplemental Figure S17.** Silencing of *NbMORF1a/1b* and *NbMORF2b/2c* affected different
601 immune signaling pathways.

602 **Supplemental Figure S18.** Sequence alignment of NbMORF2a, NbMORF2b, and NbMORF2c.
603

604 **Supplemental Table S1.** List of NbMORF family members.

605 **Supplemental Table S2.** Primers used in this study.

606

607 **Acknowledgements**

608 We thank Dr Gary J. Loake (University of Edinburgh, UK), Dr Patrick Schäfer, Dr Jim
609 Beynon, Dr Murray Grant and Dr Ruth Schäfer (University of Warwick, UK), and all lab
610 members for their insightful suggestions and encouragement. We thank Northwest A&F
611 University Life Science Research Core Services (LSRCS) for facility and technical support. This
612 work was supported by China Agriculture Research System (CARS-09), National Natural
613 Science Foundation of China (31125022 and 31930094), and the Program of Introducing Talents
614 of Innovative Discipline to Universities (project 111) from the State of Administration for
615 Foreign Experts Affairs, P. R. China (B18042).

616

617 **Figure legends**

618 **Figure 1.** MORF proteins play different immune roles in response to *Phytophthora* pathogens in
619 *Nicotiana benthamiana*. A, Silencing *NbMORF1a/1b*, *NbMORF2a*, *NbMORF2b/c*, *NbMORF8*,
620 or *NbMORF9*, respectively, in *N. benthamiana* led to different responses to *P. parasitica*. Images
621 were taken at ~40 h after inoculation with *P. parasitica* zoospores. Results were the mean \pm SE of
622 20 infections from at least 10 leaves. Statistical significance was assessed by *t* test. *** $P <$
623 0.001. Similar results were observed in three independent experiments. B, Cladogram of
624 similarities between the AtMORF (*Arabidopsis thaliana*) and NbMORF proteins. The
625 phylogenetic tree was constructed by using the neighbor-joining method. All NbMORF proteins
626 share a conserved MORF box.

627

628 **Figure 2.** Silencing *NbMORF8* attenuates cell death induced by recognition of RXLR effectors
629 of *Phytophthora* pathogens in *N. benthamiana*. A, Cell death observation of NbMORF8-silenced
630 plants and control. Images were taken at five days after *A. tumefaciens*-mediated transient
631 expression of *Avr/R* gene pairs, *INFL1*, and *Bax* on VIGS plants. B, *NbMORF8*-silenced plants
632 attenuated cell death induced by *P. parasitica* effector PpE4. C, The cell death severity
633 assessment of the *NbMORF8*-silenced leaves and control leaves. Results were the mean \pm SE of
634 at least 25 leaves from 10 plants for each group. Statistical significance was assessed by
635 Wilcoxon-Mann-Whitney test. ** $P <$ 0.01. Similar results were observed in at least six
636 independent experiments. 0, no necrosis (green); 1, necrosis area $<$ 50% of the agroinfiltrated area
637 (yellow); 2, necrosis area $>$ 50% of the agroinfiltrated area (orange). D, Quantitation of cell death.

638 0, no necrosis (green); 1, necrosis area <50% of the agroinfiltrated area (yellow); 2, necrosis area
639 >50% of the agroinfiltrated area (orange).

640 **Figure 3.** Mitochondrial and chloroplast localized MORF proteins exert opposing roles in the
641 immune response to *Phytophthora* pathogens in *N. benthamiana*. A, *P. parasitica* inoculation
642 assay on *CpNbMORF8* or *NbMORF8* overexpression leaves. Images were taken at 36 h after
643 zoospore inoculation, with *GFP* plants used as a control. The inoculated leaves were stained with
644 trypan blue to indicate the lesion area. Lesion diameter results were the mean±SE of 10
645 biological replicates. Similar results were observed in three independent experiments. Statistical
646 significance was assessed by *t* test. *** P<0.001. B, Schematic view of *NbMORF8*,
647 *dLNbMORF8*, and *CpNbMORF8*. LP, leading peptide. NLS, nuclear localization signal. dL,
648 deleting leading peptide. The leading peptide of *NbMORF8* was replaced with the *AtMORF9*
649 leading peptide to re-target the fusion proteins to the chloroplast. The *NbMORFs* were analyzed
650 using the same method. C, Subcellular localization of *NbMORF8* and *CpNbMORF8*. Confocal
651 microscopy of *N. benthamiana* leaves expressing *NbMORF8-GFP* or *CpNbMORF8-GFP*.
652 Subcellular localization was observed at 2 or 3 days post agroinfiltration (dpi). AOX-RFP was
653 used as a mitochondrial marker. Chloroplasts of *N. benthamiana* leaf cells were identified by
654 their chlorophyll autofluorescence, shown in blue. D, Mean density analysis of mitochondria and
655 chloroplasts in the subcellular localization images of *NbMORF* proteins. The three mitochondria
656 or chloroplasts showing the strongest fluorescence were analyzed from each image of *NbMORF*
657 proteins using ImageJ. Three images of each *NbMORF* were analyzed. Results were the mean
658 ±SE of nine organelles from three images. Statistical significance was assessed by *t* test. *** P <
659 0.001. E, Summary of subcellular localization and immune function of *NbMORF* proteins. √,
660 *NbMORF* protein localized. √√, *NbMORF* protein preference. -, not determined. N, chloroplast
661 localization is not required for immune function. Y, chloroplast localization is required for
662 immune function. R, resistant to *P. parasitica*. S, susceptible to *P. parasitica*.

663
664

665 **Figure 4.** Silencing *NbMORF8* up-regulated expression of defense-related genes and enhanced
666 ROS levels. A, Up-regulated expression of defense-related genes *NbPR1* and *NbPR2* in
667 *TRV-NbMORF8* plants without pathogen treatment, as determined by qPCR. B, ROS burst upon
668 flg22 treatment of *NbMORF8*-silenced leaves. At least 12 leaves from six plants of each group

669 were measured using a luminol-based chemiluminescence assay. C, The expression levels of
670 *NbPR1* and *NbPR2* in *TRV-NbMORF8* plants in the early *P. parasitica* infection stage. Total
671 RNA was extracted from *P. parasitica* zoospore-infected leaves at 3, 6, 12, and 24 h post
672 inoculation (hpi). The *N. benthamiana EF1a* gene was used as an internal control. Results were
673 the mean \pm SE. Similar results were observed in at least three independent experiments.

674
675 **Figure 5.** Silencing *NbMORF8* impaired RNA editing of *ccb206*, *cob*, and *ndhB*. A-B, The
676 editing levels of mitochondrial *ccb206* transcripts at sites 128, 148, 149, 164, 172, 193, 194, and
677 286, and *cob* at site 853, and chloroplast *ndhB* at site 242. Results were the mean \pm SE of three
678 biological replicates. Statistical significance was assessed by *t* test. * $P < 0.05$ ** $P < 0.01$. C,
679 Yeast transformants were separately transferred onto SD/-Leu/-Trp (SD-LT) and
680 SD-Leu/-Trp/-His/-Ade (SD-LTHA) medium. The growth of yeast transformants on SD-LT
681 medium demonstrated successful transformations. The growth of yeast transformants on
682 SD-LTHA indicates interactions. Image was taken three days after dropping the transformed
683 yeast on SD-LTHA medium. D, The RNA editing of *ccb206* transcripts at sites 367 and 380 was
684 down-regulated in *NbMORF8*-silenced plants during *P. parasitica* infection. Total RNA was
685 extracted from *P. parasitica* zoospore-infected leaves of *TRV-NbMORF8* and *TRV-GFP* leaves
686 at 3, 6, 12, 24, and 48 h post inoculation (hpi). Water was used as a control at each time point.
687 Results were the mean \pm SE of three biological replicates. E, The cytochrome c levels and
688 complex III activities were detected using ELISA. Results were the mean \pm SE of three biological
689 replicates. Statistical significance was assessed by *t* test. * $P < 0.05$.

690
691 **Figure 6.** The MORF box domain suppresses the immune function of *NbMORF8*. A,
692 Overexpression of *NbMORF8* mutants without the MORF box rendered plants more susceptible
693 than the full-length *NbMORF8*. Transient expression of *N-NbM8-GFP*, *dM-NbM8-GFP*,
694 *NbM8-GFP*, and *GFP* in single *N. benthamiana* leaves was done by agroinfiltration, followed by
695 inoculation with *P. parasitica* zoospores. Images were taken at 40 h after zoospore inoculation.
696 Results were the mean \pm SE of nine biological replicates. Similar results were obtained in at least
697 three independent experiments. Statistical significance was assessed by *t* test. B, Schematic view
698 of *NbMORF8* deletion mutant constructs. LP, leading peptide. N, N terminal ahead of MORF
699 box. C, C terminal behind MORF box. dC, deleting C terminal behind MORF box. dM, deleting

700 MORF box. S, susceptibility. ND, no difference compared with GFP. MS, more susceptible than
701 the full length NbMORF8. C, Subcellular localization of LP-NbMORF8, N-NbMORF8,
702 dC-NbMORF8, and dM-NbMORF8 was determined using confocal microscopy in *N.*
703 *benthamiana* leaves three days after agroinfiltration (dpi). AOX-RFP was used as a
704 mitochondrial marker. Chlorophyll fluorescence was used as chloroplast marker, shown in blue.
705 D, The yeast-two-hybrid assay of NbMORF8 mutations. Yeast transformants were separately
706 transferred onto SD/-Leu/-Trp (SD-LT) and SD-Leu/-Trp/-His/-Ade (SD-LTHA) medium. The
707 growth of yeast transformants on SD-LT medium demonstrated successful transformations, and
708 the growth of yeast transformants on SD-LTHA medium indicated interactions. Images were
709 taken five days after dropping the transformed yeast cells on SD/-LTHA medium. E, The
710 immune function of *NbMORF8* mutants was determined by transient overexpression in *N.*
711 *benthamiana* followed by inoculation with *P. parasitica* zoospores. *GFP* was used as a control.
712 The results of lesion diameter were the mean \pm SE of six biological replicates. Statistical
713 significance was assessed by *t* test. * $P < 0.05$ ** $P < 0.01$ *** $P < 0.001$. Similar results were
714 obtained in at least three independent experiments. Images were taken at 36 h after zoospore
715 inoculation for *P. parasitica*. The inoculated leaves were stained with trypan blue to show the
716 lesion area.

717 **Figure 7.** Silencing *NbMORF8* suppresses accumulation of *Phytophthora* effectors in *N.*
718 *benthamiana*. A, Sequence alignment of eGFP and TRV-GFP fragments designed for silencing.
719 B, Fluorescence intensity and eGFP accumulation in *NbMORF8*-silenced leaves. The eGFP
720 fluorescence was detected at 4 dpi. For the fluorescence intensity analysis, six pictures from each
721 group were analyzed using ImageJ. Results were the mean \pm SE of 6 pictures. Statistical
722 significance was assessed by *t* test. *** $P < 0.001$. C, Western blot of the accumulation of RXLR
723 effector proteins. Three lanes of each group indicate three biological replicates. Ponceau S
724 staining shows equal loading of protein samples. D, Semi-quantitative PCR results of effector
725 transcripts. Three lanes of each group show three biological replicates. *N. benthamiana* gene
726 *β -actin* was used to normalize equal loadings.

727

728 **Figure 8.** Schematic model for the role of *NbMORF8* in plant immunity. NbMORF8 participates
729 the RNA editing of mitochondrial genes *cob* and *ccb206*, and subsequently further affects the
730 level of cytochrome c and complex III activities. Silencing *NbMORF8* up-regulates the

731 expression of SA signal pathway markers (*NbPRI* and *NbPR2*) and ROS levels, which enhances
732 the immunity to *Phytophthora* pathogens. The *NbMORF8*-regulated ROS burst is likely achieved
733 through its effect on functionality of respiratory chain components. However, the exact ROS
734 production sites in *NbMORF8*-silenced plants remain to be revealed. *NbMORF8* is required for
735 the accumulation of multiple *Phytophthora* RXLR effectors that suppress plant immunity.
736 Mitochondrial localization of NbMORF8 is sufficient for its immune function. It remains to be
737 determined whether the potential chloroplast localization of NbMORF8 is required for plant
738 immunity or if cross-talk exists between mitochondria and chloroplasts.

739

740

741 **Literature Cited**

742

743

744

Parsed Citations

Amirsadeghi S, Robson CA, Vanlerberghe GC (2007) The role of the mitochondrion in plant responses to biotic stress. *Physiologia Plantarum* 129: 253-266

Google Scholar: [Author Only](#) [Title Only](#) [Author and Title](#)

Apel K, Hirt H (2004) Reactive oxygen species: metabolism, oxidative stress, and signal transduction. *Annual Review of Plant Biology* 55: 373-399

Google Scholar: [Author Only](#) [Title Only](#) [Author and Title](#)

Armstrong MR, Whisson SC, Pritchard L, Bos JI, Venter E, Avrova AO, Rehmany AP, Bohme U, Brooks K, Cherevach I, Hamlin N, White B, Fraser A, Lord A, Quail MA, Churcher C, Hall N, Berriman M, Huang S, Kamoun S, Beynon JL, Birch PR (2005) An ancestral oomycete locus contains late blight avirulence gene *Avr3a*, encoding a protein that is recognized in the host cytoplasm. *Proceedings of the National Academy of Sciences, USA* 102: 7766-7771

Google Scholar: [Author Only](#) [Title Only](#) [Author and Title](#)

Barkan A, Small I (2014) Pentatricopeptide repeat proteins in plants. *Annual Review of Plant Biology* 65: 415-442

Google Scholar: [Author Only](#) [Title Only](#) [Author and Title](#)

Bayer-Csaszar E, Haag S, Jorg A, Glass F, Hartel B, Obata T, Meyer EH, Brennicke A, Takenaka M (2017) The conserved domain in MORF proteins has distinct affinities to the PPR and E elements in PPR RNA editing factors. *Biochimica et Biophysica Acta - Gene Regulatory Mechanisms* 1860: 813-828

Google Scholar: [Author Only](#) [Title Only](#) [Author and Title](#)

Bentolila S, Heller WP, Sun T, Babina AM, Friso G, van Wijk KJ, Hanson MR (2012) RIP1, a member of an Arabidopsis protein family, interacts with the protein RARE1 and broadly affects RNA editing. *Proceedings of the National Academy of Sciences, USA* 109: E1453-E1461

Google Scholar: [Author Only](#) [Title Only](#) [Author and Title](#)

Bentolila S, Oh J, Hanson MR, Bukowski R (2013) Comprehensive high-resolution analysis of the role of an Arabidopsis gene family in RNA editing. *PLoS Genetics* 9: e1003584

Google Scholar: [Author Only](#) [Title Only](#) [Author and Title](#)

Block A, Guo M, Li G, Elowsky C, Clemente TE, Alfano JR (2010) The *Pseudomonas syringae* type III effector HopG1 targets mitochondria, alters plant development and suppresses plant innate immunity. *Cellular Microbiology* 12: 318-330

Google Scholar: [Author Only](#) [Title Only](#) [Author and Title](#)

Boevink PC, Wang X, McLellan H, He Q, Naqvi S, Armstrong MR, Zhang W, Hein I, Gilroy EM, Tian Z, Birch PR (2016) A *Phytophthora infestans* RXLR effector targets plant PP1c isoforms that promote late blight disease. *Nature Communications* 7: 10311

Google Scholar: [Author Only](#) [Title Only](#) [Author and Title](#)

Bottin A, Larche L, Villalba F, Gaulin E, Esquerré-Tugayé M-T, Rickauer M (1999) Green fluorescent protein (GFP) as gene expression reporter and vital marker for studying development and microbe-plant interaction in the tobacco pathogen *Phytophthora parasitica* var. *nicotianae*. *FEMS Microbiology Letters* 176: 51-56

Google Scholar: [Author Only](#) [Title Only](#) [Author and Title](#)

Brehme N, Bayer-Csaszar E, Glass F, Takenaka M (2015) The DYW subgroup PPR protein MEF35 targets RNA editing sites in the mitochondrial *rpl16*, *nad4* and *cob* mRNAs in *Arabidopsis thaliana*. *PLoS One* 10: e0140680

Google Scholar: [Author Only](#) [Title Only](#) [Author and Title](#)

Chateigner-Boutin AL, Small I (2007) A rapid high-throughput method for the detection and quantification of RNA editing based on high-resolution melting of amplicons. *Nucleic Acids Res* 35: e114

Google Scholar: [Author Only](#) [Title Only](#) [Author and Title](#)

Clark SM, Di Leo R, Dhanoa PK, Van Cauwenberghe OR, Mullen RT, Shelp BJ (2009) Biochemical characterization, mitochondrial localization, expression, and potential functions for an *Arabidopsis* gamma-aminobutyrate transaminase that utilizes both pyruvate and glyoxylate. *Journal of Experimental Botany* 60: 1743-1757

Google Scholar: [Author Only](#) [Title Only](#) [Author and Title](#)

Claros MG, Vincens P (1996) Computational method to predict mitochondrially imported proteins and their targeting sequences. *European journal of biochemistry* 241: 779-786

Google Scholar: [Author Only](#) [Title Only](#) [Author and Title](#)

Colombatti F, Gonzalez DH, Welchen E (2014) Plant mitochondria under pathogen attack: a sigh of relief or a last breath? *Mitochondrion* 19 Pt B: 238-244

Google Scholar: [Author Only](#) [Title Only](#) [Author and Title](#)

de Torres Zabala M, Littlejohn G, Jayaraman S, Studholme D, Bailey T, Lawson T, Tillich M, Licht D, Bolter B, Delfino L, Truman W, Mansfield J, Smirnov N, Grant M (2015) Chloroplasts play a central role in plant defence and are targeted by pathogen effectors. *Nature Plants* 1: 15074

Google Scholar: [Author Only](#) [Title Only](#) [Author and Title](#)

Emanuelsson O, Nielsen H, Brunak S, von Heijne G (2000) Predicting subcellular localization of proteins based on their N-terminal amino acid sequence. *Journal of Molecular Biology* 300: 1005-1016

Google Scholar: [Author Only](#) [Title Only](#) [Author and Title](#)

Foster SJ, Park T-H, Pei M, Brigneti G, Śliwka J, Jagger L, van der Vossen E, Jones JDG (2009) Rpi-vnt1.1, a Tm-22 homolog from *Solanum venturii*, confers resistance to potato late blight. *Molecular Plant-Microbe Interactions* 22: 589-600

Google Scholar: [Author Only](#) [Title Only](#) [Author and Title](#)

Garcia-Andrade J, Ramirez V, Lopez A, Vera P (2013) Mediated plastid RNA editing in plant immunity. *PLoS Pathogens* 9: e1003713

Google Scholar: [Author Only](#) [Title Only](#) [Author and Title](#)

Glass F, Hartel B, Zehrmann A, Verbitskiy D, Takenaka M (2015) MEF13 requires MORF3 and MORF8 for RNA editing at eight targets in mitochondrial mRNAs in *Arabidopsis thaliana*. *Molecular Plant* 8: 1466-1477

Google Scholar: [Author Only](#) [Title Only](#) [Author and Title](#)

Gleave AP (1992) A versatile binary vector system with a T-DNA organisational structure conducive to efficient integration of cloned DNA into the plant genome. *Plant Molecular Biology* 20: 1203-1207

Google Scholar: [Author Only](#) [Title Only](#) [Author and Title](#)

Gray MW, Covello PS (1993) RNA editing in plant mitochondria and chloroplasts. *The FASEB Journal* 7: 64-71

Google Scholar: [Author Only](#) [Title Only](#) [Author and Title](#)

Haag S, Schindler M, Berndt L, Brennicke A, Takenaka M, Weber G (2017) Crystal structures of the *Arabidopsis thaliana* organellar RNA editing factors MORF1 and MORF9. *Nucleic Acids Research* 45: 4915-4928

Google Scholar: [Author Only](#) [Title Only](#) [Author and Title](#)

Hackett JB, Shi X, Kobylarz AT, Lucas MK, Wessendorf RL, Hines KM, Bentolila S, Hanson MR, Lu Y (2017) An organelle RNA recognition motif protein is required for photosystem II subunit psbF Transcript Editing. *Plant Physiology* 173: 2278-2293

Google Scholar: [Author Only](#) [Title Only](#) [Author and Title](#)

Hartel B, Zehrmann A, Verbitskiy D, van der Merwe JA, Brennicke A, Takenaka M (2013) MEF10 is required for RNA editing at nad2-842 in mitochondria of *Arabidopsis thaliana* and interacts with MORF8. *Plant Molecular Biology* 81: 337-346

Google Scholar: [Author Only](#) [Title Only](#) [Author and Title](#)

He P, Xiao G, Liu H, Zhang L, Zhao L, Tang M, Huang S, An Y, Yu J (2018) Two pivotal RNA editing sites in the mitochondrial atp1 mRNA are required for ATP synthase to produce sufficient ATP for cotton fiber cell elongation. *New Phytologist* 218: 167-182

Google Scholar: [Author Only](#) [Title Only](#) [Author and Title](#)

Huang G, Liu Z, Gu B, Zhao H, Jia J, Fan G, Meng Y, Du Y, Shan W (2019) An RXLR effector secreted by *Phytophthora parasitica* is a virulence factor and triggers cell death in various plants. *Molecular Plant Pathology* 20: 356-371

Google Scholar: [Author Only](#) [Title Only](#) [Author and Title](#)

Huang S, Van Der Vossen EAG, Kuang H, Vleeshouwers VGAA, Zhang N, Borm TJA, Van Eck HJ, Baker B, Jacobsen E, Visser RGF (2005) Comparative genomics enabled the isolation of the R3a late blight resistance gene in potato. *Plant Journal* 42: 251-261

Google Scholar: [Author Only](#) [Title Only](#) [Author and Title](#)

Itani K, Handa H (1998) Rapeseed mitochondrial ccb206, a gene involved in cytochrome c biogenesis, is co-transcribed with the nad3 and rps12 genes: organization, transcription, and RNA editing of the nad3/rps12/ccb206 locus. *Current Genetics* 34: 318-325

Google Scholar: [Author Only](#) [Title Only](#) [Author and Title](#)

Jia J (2017) Diversity of small RNAs and their potential roles in the regulation of gene expression in *Phytophthora parasitica*. PhD thesis. Northwest A&F University.

Google Scholar: [Author Only](#) [Title Only](#) [Author and Title](#)

Jones JD, Dangl JL (2006) The plant immune system. *Nature* 444: 323-329

Google Scholar: [Author Only](#) [Title Only](#) [Author and Title](#)

Kamoun S, Furzer O, Jones JD, Judelson HS, Ali GS, Dalio RJ, Roy SG, Schena L, Zambounis A, Panabieres F, Cahill D, Ruocco M, Figueiredo A, Chen XR, Hulvey J, Stam R, Lamour K, Gijzen M, Tyler BM, Grunwald NJ, Mukhtar MS, Tome DF, Tor M, Van Den Ackerveken G, McDowell J, Daayf F, Fry WE, Lindqvist-Kreuzer H, Meijer HJ, Petre B, Ristaino J, Yoshida K, Birch PR, Govers F (2015) The top 10 oomycete pathogens in molecular plant pathology. *Molecular Plant Pathology* 16: 413-434

Google Scholar: [Author Only](#) [Title Only](#) [Author and Title](#)

Koprivova A, des Francs-Small CC, Calder G, Mugford ST, Tanz S, Lee BR, Zehrmann B, Small I, Kopriva S (2010) Identification of a pentatricopeptide repeat protein implicated in splicing of intron 1 of mitochondrial nad7 transcripts. *Journal of Biological Chemistry* 285: 32192-32199

Google Scholar: [Author Only](#) [Title Only](#) [Author and Title](#)

Kumar S, Stecher G, Tamura K (2016) MEGA7: molecular evolutionary genetics analysis version 7.0 for bigger datasets. *Molecular Biology and Evolution* 33: 1870-1874

Google Scholar: [Author Only](#) [Title Only](#) [Author and Title](#)

Li T, Wang Q, Feng R, Li L, Ding L, Fan G, Li W, Du Y, Zhang M, Huang G, Schäfer P, Meng Y, Tyler BM, Shan W (2019) Negative regulators of plant immunity derived from a non-ribosomal adenosine hydrolase are targeted by multiple *Phytophthora* Avr3a-like

effectors. *New Phytologist*: doi: 10.1111/nph.16139

Google Scholar: [Author Only](#) [Title Only](#) [Author and Title](#)

Ma F, Hu Y, Ju Y, Jiang Q, Cheng Z, Zhang Q, Sodmergen (2017) A novel tetratricopeptide repeat protein, WHITE TO GREEN1, is required for early chloroplast development and affects RNA editing in chloroplasts. *Journal of Experimental Botany* 68: 5829-5843

Google Scholar: [Author Only](#) [Title Only](#) [Author and Title](#)

McLellan H, Boevink PC, Armstrong MR, Pritchard L, Gomez S, Morales J, Whisson SC, Beynon JL, Birch PR (2013) An RxLR effector from *Phytophthora infestans* prevents re-localisation of two plant NAC transcription factors from the endoplasmic reticulum to the nucleus. *PLoS Pathogens* 9: e1003670

Google Scholar: [Author Only](#) [Title Only](#) [Author and Title](#)

Mittler R, Vanderauwera S, Gollery M, Van Breusegem F (2004) Reactive oxygen gene network of plants. *Trends in Plant Science* 9: 490-498

Google Scholar: [Author Only](#) [Title Only](#) [Author and Title](#)

Møller IM (2001) Plant mitochondria and oxidative stress: electron transport, NADPH turnover, and metabolism of reactive oxygen species. *Annual Review of Plant Physiology and Plant Molecular Biology* 52: 561-592

Google Scholar: [Author Only](#) [Title Only](#) [Author and Title](#)

Narsai R, Law SR, Carrie C, Xu L, Whelan J (2011) In-depth temporal transcriptome profiling reveals a crucial developmental switch with roles for RNA processing and organelle metabolism that are essential for germination in *Arabidopsis*. *Plant Physiology* 157: 1342-1362

Google Scholar: [Author Only](#) [Title Only](#) [Author and Title](#)

Nomura H, Komori T, Uemura S, Kanda Y, Shimotani K, Nakai K, Furuichi T, Takebayashi K, Sugimoto T, Sano S, Suwastika IN, Fukusaki E, Yoshioka H, Nakahira Y, Shiina T (2012) Chloroplast-mediated activation of plant immune signalling in *Arabidopsis*. *Nature Communications* 3: 926

Google Scholar: [Author Only](#) [Title Only](#) [Author and Title](#)

Pan Q, Cui B, Deng F, Quan J, Loake GJ, Shan W (2016) RTP1 encodes a novel endoplasmic reticulum (ER)-localized protein in *Arabidopsis* and negatively regulates resistance against biotrophic pathogens. *New Phytologist* 209: 1641-1654

Google Scholar: [Author Only](#) [Title Only](#) [Author and Title](#)

Pel MA, Foster SJ, Park T-H, Rietman H, van Arkel G, Jones JDG, Van Eck HJ, Jacobsen E, Visser RGF, Van der Vossen EAG (2009) Mapping and cloning of late blight resistance genes from *Solanum venturii* using an interspecific candidate gene approach. *Molecular Plant-Microbe Interactions* 22: 601-615

Google Scholar: [Author Only](#) [Title Only](#) [Author and Title](#)

Rodriguez-Herva JJ, Gonzalez-Melendi P, Cuartas-Lanza R, Antunez-Lamas M, Rio-Alvarez I, Li Z, Lopez-Torrejon G, Diaz I, Del Pozo JC, Chakravarthy S, Collmer A, Rodriguez-Palenzuela P, Lopez-Solanilla E (2012) A bacterial cysteine protease effector protein interferes with photosynthesis to suppress plant innate immune responses. *Cellular Microbiology* 14: 669-681

Google Scholar: [Author Only](#) [Title Only](#) [Author and Title](#)

Saitou N, Nei M (1987) The neighbor-joining method: a new method for reconstructing phylogenetic trees. *Molecular Biology and Evolution* 4: 406-425

Google Scholar: [Author Only](#) [Title Only](#) [Author and Title](#)

Sandoval R, Boyd RD, Kiszter AN, Mirzakhanyan Y, Santibanez P, Gershon PD, Hayes ML (2019) Stable native RIP9 complexes associate with C-to-U RNA editing activity, PPRs, RIPs, OZ1, ORRM1 and ISE2. *Plant Journal* 99: 1116-1126

Google Scholar: [Author Only](#) [Title Only](#) [Author and Title](#)

Sang Y, Macho AP (2017) Analysis of PAMP-triggered ROS burst in plant immunity. *Methods in Molecular Biology* 1578: 143-153

Google Scholar: [Author Only](#) [Title Only](#) [Author and Title](#)

Schwessinger B, Ronald PC (2012) Plant innate immunity: perception of conserved microbial signatures. *Annual Review of Plant Biology* 63: 451-482

Google Scholar: [Author Only](#) [Title Only](#) [Author and Title](#)

Senthil-Kumar M, Mysore KS (2014) Tobacco rattle virus-based virus-induced gene silencing in *Nicotiana benthamiana*. *Nature Protocols* 9: 1549-1562

Google Scholar: [Author Only](#) [Title Only](#) [Author and Title](#)

Serrano I, Audran C, Rivas S (2016) Chloroplasts at work during plant innate immunity. *Journal of Experimental Botany* 67: 3845-3854

Google Scholar: [Author Only](#) [Title Only](#) [Author and Title](#)

Shi X, Hanson MR, Bentolila S (2015) Two RNA recognition motif-containing proteins are plant mitochondrial editing factors. *Nucleic Acids Res* 43: 3814-3825

Google Scholar: [Author Only](#) [Title Only](#) [Author and Title](#)

Shikanai T (2015) RNA editing in plants: machinery and flexibility of site recognition. *Biochimica et Biophysica Acta* 1847: 779-785

Google Scholar: [Author Only](#) [Title Only](#) [Author and Title](#)

Song J, Bradeen JM, Naess SK, Raasch JA, Wielgus SM, Haberlach GT, Liu J, Kuang H, Austin-Phillips S, Buell CR, Helgeson JP, Jiang J (2003) Gene RB cloned from *Solanum bulbocastanum* confers broad spectrum resistance to potato late blight. *Proceedings of the National Academy of Sciences, USA* 100: 9128–9133.

Google Scholar: [Author Only](#) [Title Only](#) [Author and Title](#)

Sperschneider J, Catanzariti AM, DeBoer K, Petre B, Gardiner DM, Singh KB, Dodds PN, Taylor JM (2017) LOCALIZER: subcellular localization prediction of both plant and effector proteins in the plant cell. *Scientific Reports* 7: 44598

Google Scholar: [Author Only](#) [Title Only](#) [Author and Title](#)

Sun T, Bentolila S, Hanson MR (2016) The unexpected diversity of plant organelle RNA editosomes. *Trends in Plant Science* 21: 962-973

Google Scholar: [Author Only](#) [Title Only](#) [Author and Title](#)

Sun T, Shi X, Friso G, Van Wijk K, Bentolila S, Hanson MR (2015) A zinc finger motif-containing protein is essential for chloroplast RNA editing. *PLoS Genetics* 11: e1005028

Google Scholar: [Author Only](#) [Title Only](#) [Author and Title](#)

Takenaka M, Zehrmann A, Verbitskiy D, Hartel B, Brennicke A (2013) RNA editing in plants and its evolution. *Annual Review of Genetics* 47: 335-352

Google Scholar: [Author Only](#) [Title Only](#) [Author and Title](#)

Takenaka M, Zehrmann A, Verbitskiy D, Kugelman M, Hartel B, Brennicke A (2012) Multiple organellar RNA editing factor (MORF) family proteins are required for RNA editing in mitochondria and plastids of plants. *Proceedings of the National Academy of Sciences, USA* 109: 5104-5109

Google Scholar: [Author Only](#) [Title Only](#) [Author and Title](#)

Vleeshouwers VGAA, Rietman H, Krenek P, Champouret N, Young C, Oh S-K, Wang M, Bouwmeester K, Vosman B, Visser RGF, Jacobsen E, Govers F, Kamoun S, Van der Vossen EAG (2008) Effector genomics accelerates discovery and functional profiling of potato disease resistance and *Phytophthora infestans* avirulence genes. *PLoS ONE* 3: e2875

Google Scholar: [Author Only](#) [Title Only](#) [Author and Title](#)

Wang Y, Bouwmeester K, van de Mortel JE, Shan W, Govers F (2013) A novel *Arabidopsis*-oomycete pathosystem: differential interactions with *Phytophthora capsici* reveal a role for camalexin, indole glucosinolates and salicylic acid in defence. *Plant, Cell and Environment* 36: 1192-1203

Google Scholar: [Author Only](#) [Title Only](#) [Author and Title](#)

Wang Y, Meng Y, Zhang M, Tong X, Wang Q, Sun Y, Quan J, Govers F, Shan W (2011) Infection of *Arabidopsis thaliana* by *Phytophthora parasitica* and identification of variation in host specificity. *Molecular Plant Pathology* 12: 187-201

Google Scholar: [Author Only](#) [Title Only](#) [Author and Title](#)

Weiss H (1987) Structure of Mitochondrial Ubiquinol–Cytochrome-c Reductase (Complex III). *Current Topics in Bioenergetics* 15: 67-90

Google Scholar: [Author Only](#) [Title Only](#) [Author and Title](#)

Wesley SV, Helliwell CA, Smith NA, Wang MB, Rouse DT, Liu Q, Gooding PS, Singh SP, Abbott D, Stoutjesdijk PA, Robinson SP, Gleave AP, Green AG, Waterhouse PM (2001) Construct design for efficient, effective and high-throughput gene silencing in plants. *Plant Journal* 27: 581-590

Google Scholar: [Author Only](#) [Title Only](#) [Author and Title](#)

Yan J, Zhang Q, Yin P (2017) RNA editing machinery in plant organelles. *Science China Life Sciences* 61: 162-169

Google Scholar: [Author Only](#) [Title Only](#) [Author and Title](#)

Yan Q, Cui X, Lin S, Gan S, Xing H, Dou D (2016) GmCYP82A3, a Soybean cytochrome P450 family gene involved in the jasmonic acid and ethylene signaling pathway, enhances plant resistance to biotic and abiotic stresses. *PLoS One* 11: e0162253

Google Scholar: [Author Only](#) [Title Only](#) [Author and Title](#)

Yang L, McLellan H, Naqvi S, He Q, Boevink PC, Armstrong M, Giuliani LM, Zhang W, Tian Z, Zhan J, Gilroy EM, Birch PR (2016) Potato NPH3/RPT2-like protein StNRL1, targeted by a *Phytophthora infestans* RXLR effector, is a susceptibility factor. *Plant Physiology* 171: 645-657

Google Scholar: [Author Only](#) [Title Only](#) [Author and Title](#)

Yang Y, Zhu G, Li R, Yan S, Fu D, Zhu B, Tian H, Luo Y, Zhu H (2017) The RNA editing factor SIORRM4 is required for normal fruit ripening in tomato. *Plant Physiology* 175: 1690-1702

Google Scholar: [Author Only](#) [Title Only](#) [Author and Title](#)

Zehrmann A, Hartel B, Glass F, Bayer-Csaszar E, Obata T, Meyer E, Brennicke A, Takenaka M (2015) Selective homo- and heteromer interactions between the multiple organellar RNA editing factor (MORF) proteins in *Arabidopsis thaliana*. *Journal of Biological Chemistry* 290: 6445-6456

Google Scholar: [Author Only](#) [Title Only](#) [Author and Title](#)

Zhang F, Tang W, Hedtke B, Zhong L, Liu L, Peng L, Lu C, Grimm B, Lin R (2014) Tetrapyrrole biosynthetic enzyme protoporphyrinogen IX oxidase 1 is required for plastid RNA editing. *Proceedings of the National Academy of Sciences, USA* 111: 2023-2028

Google Scholar: [Author Only](#) [Title Only](#) [Author and Title](#)

Zhao X, Huang J, Chory J (2019) GUN1 interacts with MORF2 to regulate plastid RNA editing during retrograde signaling. *Proceedings of the National Academy of Sciences, USA* 116:10162-10167.

Google Scholar: [Author Only](#) [Title Only](#) [Author and Title](#)

Zhu Q, Dugardeyn J, Zhang C, Takenaka M, Kuhn K, Craddock C, Smalle J, Karampelias M, Denecke J, Peters J, Gerats T, Brennicke A, Eastmond P, Meyer EH, Van Der Straeten D (2012) SLO2, a mitochondrial pentatricopeptide repeat protein affecting several RNA editing sites, is required for energy metabolism. *Plant J* 71: 836-849

Google Scholar: [Author Only](#) [Title Only](#) [Author and Title](#)

Zsigmond L, Rigo G, Szarka A, Szekely G, Otvos K, Darula Z, Medzihradzsky KF, Koncz C, Koncz Z, Szabados L (2008) Arabidopsis PPR40 connects abiotic stress responses to mitochondrial electron transport. *Plant Physiology* 146: 1721-1737

Google Scholar: [Author Only](#) [Title Only](#) [Author and Title](#)